Title:
What is the contribution of human FMO3 in the N-oxygenation of selected therapeutic drugs and drugs of abuse?

Authors:
Lea Wagmann, Markus R. Meyer, Hans H. Maurer

This is the accepted manuscript of an article published in *Toxicology Letters* (Volume 258, 6 September 2016, Pages 55-70, DOI: 10.1016/j.toxlet.2016.06.013).

The version of record is available online at: https://doi.org/10.1016/j.toxlet.2016.06.013

What is the contribution of human FMO3 in the *N*-oxygenation of selected therapeutic drugs and drugs of abuse?

Lea Wagmann[a], Markus R. Meyer[ab], and Hans H. Maurer[a*]

[a]*Department of Experimental and Clinical Toxicology, Saarland University, Homburg, Germany*

[b]*Department of Clinical Pharmacology and Pharmacoepidemiology, Heidelberg University Hospital, Heidelberg, Germany*

---

*Corresponding author.

E-mail address: hans.maurer@uks.eu (H.H. Maurer).

ABSTRACT

Little is known about the role of flavin-containing monooxygenases (FMOs) in the metabolism of xenobiotics. FMO3 is the isoform in adult human liver with the highest impact on drug metabolism. The aim of the presented study was to elucidate the contribution of human FMO3 to the *N*-oxygenation of selected therapeutic drugs and drugs of abuse (DOAs). Its contribution to the in vivo hepatic net clearance of the *N*-oxygenation products was calculated by application of an extended relative activity factor (RAF) approach to differentiate from contribution of cytochrome P450 (CYP) isoforms. FMO3 and CYP substrates were identified using pooled human liver microsomes after heat inactivation and chemical inhibition, or single enzyme incubations. Kinetic parameters were subsequently determined using recombinant human enzymes and mass spectrometric analysis via authentic reference standards or simple peak areas of the products divided by those of the internal standard. FMO3 was identified as enzyme mainly responsible for the formation of *N,N*-diallyltryptamine *N*-oxide and methamphetamine hydroxylamine (> 80% contribution for both). A contribution of 50 and 30% was calculated for the formation of *N,N*-dimethyltryptamine *N*-oxide and methoxypiperamide *N*-oxide, respectively. However, FMO3 contributed with less than 5% to the formation of 3-bromomethcathinone hydroxylamine, amitriptyline *N*-oxide, and clozapine *N*-oxide. There was no significant difference in the contributions when using calibrations with reference metabolite standards or peak area ratio calculations. The successful application of a modified RAF approach including FMO3 proved the importance of FMO3 in the *N*-oxygenation of DOAs in human metabolism.

Keywords FMO3, CYPs, Drugs of abuse, Relative activity factor approach, Hepatic clearance

1. Introduction

Monooxygenases are responsible for the major part of the human phase I metabolism and convert xenobiotics to more hydrophilic compounds usually leading to inactivation (Cashman, 2005; Zollner *et al.*, 2010). These monooxygenases can be grouped into different enzyme families such as the cytochrome P450 monooxygenases (CYPs) and the flavin-containing monooxygenases (FMOs) (Torres Pazmino *et al.*, 2010). CYPs catalyze oxygenation mainly of carbon but also of nitrogen and sulfur. FMOs usually oxygenate soft nucleophiles, in particular nitrogen, sulfur, phosphorous, and selenium atoms. Both microsomal systems have in common, that they transform a wide range of heteroatom-containing substrates (Cashman, 2005; Cruciani *et al.*, 2014).

In comparison to the extensively studied CYPs, FMOs have long been neglected in metabolism investigations. In addition, experimental conditions were usually chosen to optimize CYP activity rather than the activity of other oxidative enzymes leading to underestimation of non-CYP reactions (Strolin *et al.*, 2006). Recently, Fan et al. asked for further investigations that dissect the relative contribution of FMOs compared to CYPs (Fan *et al.*, 2016). Hence, only limited information about interactions of FMO with therapeutic drugs and drugs of abuse (DOAs) in particular is available. Only the oxygenation of amphetamine and methamphetamine by human FMO was described so far, leading to reactive metabolites (Cashman *et al.*, 1999; Szoko *et al.*, 2004). Cashman et al. reported that amphetamine and methamphetamine were *N*-oxygenated by FMO3, the major FMO isoform in the adult human liver. The formed hydroxylamines were also identified as FMO3 substrates leading to *N,N*-dihydroxylation followed by conversion to phenylpropanone oxime and phenylpropanone, respectively. Particularly the first step may pose a significant toxicological threat due to the potential toxic nature of free hydroxylamine (Cashman *et al.*, 1999).

Therefore, the aim of the presented study was to elucidate the contribution of FMO3 to the human, hepatic metabolism of 12 selected, structurally different therapeutic drugs and eight DOAs. Its contribution to the in vivo hepatic net clearance of the *N*-oxygenation products should be calculated by application of an extended relative activity factor (RAF) approach (Crespi and Miller, 1999; Venkatakrishnan *et al.*, 2001) to differentiate from contribution of CYP isoforms. Finally, possible differences in the

contributions should be assessed by using calibrations with reference metabolite standards or peak area ratio (PAR) calculations.

2. Materials and methods

2.1. Chemicals and enzymes

Dimethyltryptamine (DMT) was obtained from THC Pharm (Frankfurt, Germany), methadone from Lipomed (Weil am Rhein, Germany), trimipramine-d_3 and norclozapine-d_8 from Promochem (Wesel, Germany), *R,S*-methamphetamine, 1-aminobenzotriazole (ABT), isocitrate (IC), isocitrate dehydrogenase (IDH), superoxide dismutase (SOD), potassium dihydrogenphosphate (KH_2PO_4), and dipotassium hydrogenphosphate (K_2HPO_4) from Sigma-Aldrich (Taufkirchen, Germany). All other used drugs (of abuse) were supplied by commercial suppliers (e.g. Fluka, Neu Ulm, Germany; LG Chemicals, Teddington, UK; Lipomed, Weil am Rhein, Germany; Promochem, Wesel, Germany) or by the manufacturers of the marketed drugs. $NADP^+$ was from Biomol (Hamburg, Germany), formic acid (MS grade) from Fluka (Neu-Ulm, Germany), acetonitrile, methanol (both LC–MS grade), and all other chemicals from VWR (Darmstadt, Germany). Methanolic stock solutions (1 mg/mL) of the studied compounds were used. The chemical structures of all tested DOAs are depicted in Fig. 1.

The baculovirus-infected insect cell microsomes (Supersomes) containing human complementary DNA-expressed FMO3 (5 mg protein/mL), CYP1A2, CYP2A6, CYP2B6, CYP2C8, CYP2C9, CYP2C19, CYP2D6, CYP3A4 (1 nmol/mL), or CYP2E1, CYP3A5 (2 nmol/mL), and pooled human liver microsomes (pHLM, 20 mg microsomal protein/mL, 330 pmol total CYP/mg protein) were obtained from Corning (Amsterdam, The Netherlands). After delivery, the microsomes were thawed at 37°C, aliquoted, snap-frozen in liquid nitrogen, and stored at -80°C until use.

2.2. pHLM incubations

Incubations were performed at 37°C for 30 min with 25 µM of the substrate, regenerating system, and 1 mg protein/mL pHLM according to (Michely *et al.*, 2015). Incubations with pHLM were done without pretreatment, after preincubation with the chemical inhibitors ABT (2 mM) for CYPs or methimazole (200 µM) for FMOs, or after preheating. Heat-treated pHLM were prepared by heating at 55°C for 1 min in absence of $NADP^+$ in accordance to Ring et al. (Ring *et al.*, 1999) or at 45°C for 5 min in absence of $NADP^+$ and cooling on ice for 15 min in accordance to Taniguchi-Takizawa et al. (Taniguchi-Takizawa *et al.*, 2015). In addition, blank incubations with buffer instead of enzymes were performed. As described before (Michely *et al.*, 2015), besides enzymes and substrate, the incubation mixtures (final volume 50 µL) contained 90 mM phosphate buffer (pH 7.4), 5 mM Mg^{2+}, 5 mM IC, 1.2 mM $NADP^+$, 0.5 U/mL IDH, and 200 U/mL SOD. Reactions were initiated by addition of the substrate and stopped with 50 µL of ice-cold acetonitrile, containing 5 µM internal standard. Trimipramine-d_3 was used as internal standard for incubations with all analytes, except for amitriptyline, where norclozapine-d_8 was used. The solution was centrifuged for 5 min at 14,000×*g*, 70 µL of the supernatant phase was transferred to an autosampler vial and 10 µL injected onto the liquid chromatography (LC)-ion trap (IT)-mass spectrometry (MS) system described below. The amounts of formed metabolites in untreated and pretreated incubations were compared by calculating the PAR of the metabolites and the internal standard. All incubations were performed in duplicate (n = 2).

2.3. Monooxygenases Activity Screening

Incubation mixtures contained 25 µM of the test substrate and FMO3 (0.25 mg protein/mL), CYP1A2, CYP2A6, CYP2B6, CYP2C8, CYP2C9, CYP2C19, CYP2D6, CYP2E1, CYP3A4, CYP3A5 (50 pmol/mL, each), or pHLM (1 mg protein/mL). For incubations with CYP2A6 or CYP2C9, phosphate buffer was replaced with 45 or 90 mM Tris buffer, respectively, according to the Gentest manual. Incubations were conducted as described in 2.2.

2.4. Kinetic studies

The kinetic constants of *N*-oxygenation reactions were derived from incubations with FMO3, single CYPs, or pHLM. Incubation time and enzyme concentration were always set in the linear range of metabolite formation. Substrate concentrations were chosen to allow modeling of enzyme kinetics and were usually between 1 and 2000 µM. The concentration of organic solvent was always ≤ 2% (Chauret *et al.*, 1998). All incubations were performed in triplicate (n = 3). Kinetic constants were calculated via two ways: (a) quantification of the formed products by calibration using the corresponding reference standards (CRS, different concentrations between 0.001 and 1 µM, non-linear regression, either no weighting or weighted ($1/x^2$, where x is the CRS concentration), depending on investigated substrate and enzyme), (b) the peak areas of the products divided by those of the internal standard amitriptyline *N*-oxide (used for clozapine kinetics) or clozapine *N*-oxide (used for kinetics of all other analytes), respectively. These PARs were used instead of concentrations for calculating the enzyme kinetic constants.

Enzyme kinetic constants were estimated by nonlinear curve fitting using GraphPad Prism 5.00 software (GraphPad Software, San Diego, USA). The Michaelis-Menten equation (Eq. (1)) was used to calculate apparent K_m and V_{max} values for single-enzyme systems and pHLM.

(1) $$V = \frac{V_{max}\, x\, [S]}{K_m + [S]}$$

2.5. Calculation of relative activity factors, contributions, and percentages of net clearance

The RAF approach (Crespi and Miller, 1999; Stormer *et al.*, 2000) was based on the hypothesis that the human liver microsomal rates of a biotransformation mediated by multiple CYP isoforms could be mathematically reconstructed from the rates of the biotransformation catalyzed by individual recombinant CYPs (Venkatakrishnan *et al.*, 2001). It was used for the in vitro-in vivo scaling of pharmacokinetic clearance from in vitro intrinsic clearance measurements in heterologous expression systems (Venkatakrishnan *et al.*, 2001).

The turnover rates (TR) of FMO3 (probe substrate (PS) methyl p-tolyl sulfide), CYP1A2 (PS phenacetin), CYP2B6 (PS 7-ethoxy-4-trifluromethylcoumarin), CYP2C8

(PS paclitaxel), CYP2C19 (PS S-mephenytoin), CYP2D6 (PS bufuralol), CYP2E1 (PS chlorzoxazone), and CYP3A4 (PS testosterone) in insect cell microsomes (ICM) and pHLM were taken from the supplier's data sheets. The RAFs were calculated according to Eq. (2).

(2) $$RAF_{enzyme} = \frac{TR_{PS}\ in\ pHLM}{TR_{PS}\ in\ ICM}$$

The enzyme velocities V_{enzyme} (see Eq. (1)) for the respective metabolic reactions were calculated at different substrate concentrations and multiplied by the corresponding RAF leading to a value, which was defined as 'contribution' (Eq. (3)). The K_m and V_{max} values (Eq. (1)) were obtained from the incubations with cDNA-expressed enzymes.

(3) $$contribution_{enzyme} = RAF_{enzyme}\, x\, V_{enzyme}$$

Based on these corrected activities (contributions) the percentages of net clearance by a particular enzyme at a certain substrate concentration can be calculated using Eq. (4).

(4) $$clearance_{enzyme}[\%] = \frac{contribution_{enzyme}}{\sum contribution_{enzyme}} x\ 100$$

2.6. Apparatus and LC-conditions

All samples were analyzed using a ThermoFisher Scientific (TF, Dreieich, Germany) LXQ linear IT-MS, coupled to a TF Accela ultra high performance LC (UHPLC) system consisting of a degasser, a quaternary pump, and an autosampler. Gradient elution was performed on a TF Hypersil GOLD C18 column (100×2.1 mm, 1.9 µm). The mobile phase consisted of 10 mM aqueous ammonium formate plus 0.1% formic acid (pH 3.4, eluent A) and acetonitrile plus 0.1% formic acid (eluent B). The flow rate was set to 0.6 mL/min and the following gradient was used: 0-7.5 min to 5% A, 7.5-10.0 min hold 5% A, 10.0-11.5 min to 98% A, 11.5-15.0 min hold 98% A. For separation of amitriptyline and its *N*-oxide, the flow rate was set to 0.5 mL/min and the gradient was programmed as follows: 0–1.0 min 98% A, 1.0–3.0 min to 90% A,

3.0–5.0 min to 85% A, 5.0–7.5 min to 80% A, 7.5–10.0 min to 75% A, 10.0–11.5 min to 70% A, 11.5–13.0 min to 65% A, 13.0–14.5 min to 50% A, 14.5–16.0 min to 40% A, 16.0– 19.0 min to 10% A, 19.0–21.0 hold 10% A, as previously described in (Wissenbach *et al.*, 2011b). Analysis was performed in full-scan mode (*m/z* 100-800) or in a targeted acquisition mode with inclusion list, where MS^2 spectra of given precursor ions were recorded. The injection volume for all samples was 10 µL each. The MS was equipped with a heated electrospray ionization II source, other conditions were as follows: positive ionization mode; sheath gas, nitrogen at flow rate of 34 arbitrary units (AU); auxiliary gas, nitrogen at flow rate of 11 AU; vaporizer temperature, 250°C; source voltage, 3.00 kV; ion transfer capillary temperature, 300°C; capillary voltage, 31 V; tube lens voltage, 110 V; automatic gain control was set to 15,000 ions for full scan and 5,000 ions for MS^n, as already described in (Wissenbach *et al.*, 2011a). Wissenbach et al. described 0.01, 0.1, or 1.0 mg/L as limits of detection determined for several DOAs (Wissenbach *et al.*, 2011a).

2.7. Data analysis

TF Xcalibur Qual Browser software version 2.2 SP1.48 was used for calculation of the peak areas for assessment of the relative amount of metabolites formed during incubation and GraphPad Prism 5.00 for statistical evaluations. T-test conditions were unpaired and one-tailed (***, $P < 0.001$, **, $P < 0.01$, *. $P < 0.1$).

3. Results

3.1. Identification of FMO substrates by heat inactivation or chemical inhibition

Incubations of 12 therapeutic drugs using untreated pHLM or preheated pHLM (55°C, 1 min) were conducted. The unchanged drugs, *N*-oxides, and nor metabolites were analyzed by LC-IT-MS. Ten out of 12 substrates formed the corresponding *N*-oxides and nor metabolites in incubations with untreated pHLM. For venlafaxine, only the nor metabolite and for ranitidine, no metabolites could be detected. Untreated pHLM incubations were used as control and the amount of metabolite formed, minus

metabolite formation in blank samples, was defined as 100%. In comparison to metabolite formation in untreated pHLM incubations, heat-treated (55°C) pHLM incubations showed a reduced formation for both metabolites each between 60 and 100% as shown in Fig. 2a. The lowest reduction was observed for the metabolites of doxepin, followed by those of amitriptyline, citalopram, prothipendyl, zolpidem, and zopiclone. For clozapine, diphenhydramine, doxylamine, and imipramine, *N*-oxygenation could not be observed.

Results of incubations with amitriptyline, clozapine, imipramine, and zopiclone with pHLM, preheated at 45°C for 5 min, are shown in Fig. 2b. Here again a reduction of the formation rates of both metabolites was observed, although less pronounced then after preincubation of pHLM at 55°C. The reduction was between 30 and 50%, except for imipramine *N*-oxide formation that was reduced by 80%. Additionally, these four therapeutic drugs were incubated with recombinant FMO3 under conditions as described in 2.3. In these incubations, nor metabolites were not formed at all.

Furthermore, amitriptyline, clozapine, imipramine, and zopiclone were incubated using pHLM preincubated with ABT or methimazole. Results are shown in Fig. 3. After preincubation with ABT (Fig. 3a), formation of the *N*-oxides of amitriptyline and clozapine was reduced by about 80%, while the *N*-oxygenation of imipramine remained unchanged and that of zopiclone was almost entirely prevented. In each case, an almost complete disappearance of the nor metabolites could be observed. After preincubation with methimazole (Fig. 3b), formation rates of both metabolites were affected and reduced between 70 and 90%. Incubations with recombinant FMO3, preincubated with ABT and regenerating system for 30 min were performed, under conditions as already described in 2.2. and 2.3. There was no difference in the *N*-oxide formation between incubations with and without ABT preincubation.

3.2. Identification of enzymes involved in the N-oxygenation

A monooxygenases activity screening using FMO3, ten CYP isoforms, or pHLM was conducted. The unchanged drugs, *N*-oxygenation products, and main metabolites (usually nor and mono hydroxy metabolites) were analyzed by LC-IT-MS. The corresponding *N*-oxygenation product was detected in all incubations with pHLM,

except for methamphetamine. While the highest amount of zopiclone *N*-oxide was detected in incubations with CYP3A4, FMO3 showed no activity. Low amounts of imipramine *N*-oxide were found in incubations with FMO3 and also CYP1A2, CYP2B6, CYP2C19, and CYP2D6. *N*-Oxide formation of amitriptyline and clozapine was observed for FMO3 and various CYP isoforms.

N-Oxygenation of the DOAs 3-bromomethcathinone (3-BMC), *N,N*-diallyltryptamine (DALT), DMT, methoxypiperamide (MeOP), and methamphetamine was catalyzed by FMO3 and some CYPs, while *N*-oxygenation of dextromethorphan, glaucine, and methadone was not catalyzed by FMO3 but by CYPs.

3.3. Kinetic studies, calculation of contributions, and hepatic clearances using a modified RAF approach

The kinetics for all *N*-oxygenations is depicted in Fig. 4 and followed classic Michaelis-Menten kinetics. The corresponding Michaelis-Menten constants are summarized in Table 1. If product inhibition was observed, high concentrations were excluded for calculations of K_m and V_{max} values. In general, CYPs showed higher affinity, represented by lower K_m values, in comparison to higher K_m values for FMO3. As pHLM contained all tested individual enzymes, resulting K_m values were between CYP and FMO3 values. FMO3 showed the highest turnover rates (V_{max}), followed by pHLM and CYPs. Calculations using CRS and PAR resulted in similar K_m values, while V_{max} values obtained by different methods could not be compared due to different units (pmol/min/mg for CRS and AU/min/mg for PAR). The RAFs for used recombinant enzymes were calculated according to Eq. (2). Turnover rates for appropriate probe substrates were taken from the supplier's data sheets. Applying the RAF approach, the contribution and in vivo hepatic net clearance was calculated with K_m and V_{max} values determined by CRS or PAR. The results for the hepatic net clearance of amitriptyline *N*-oxide at different amitriptyline concentrations are given in Fig. 5. The results for the hepatic net clearance of the *N*-oxygenation products of clozapine and five DOAs at a substrate concentration of 0.1 µM are given in Fig. 6. Results for all tested therapeutic drugs and DOAs at different substrate concentrations are given in Table 2. Concerning amitriptyline and clozapine, FMO3 played only a minor role in the hepatic *N*-oxide clearance, while various CYPs were

responsible for the major part of the *N*-oxide formation. In case of amitriptyline *N*-oxide formation, contribution showed almost equal distribution among CYP1A2, CYP2B6, and CYP2D6, while CYP3A4 was predominantly responsible for clozapine *N*-oxide formation. *N*-Oxygenation of 3-BMC showed a similar profile as amitriptyline, concerning a distribution among various CYPs and a low contribution of FMO3. For DALT and methamphetamine, only FMO3 and a single CYP isoform (CYP3A4 or CYP2D6, respectively) were involved in the *N*-oxygenation, whereby FMO3 played the predominant role with contributions > 80% to the hepatic clearances. For DMT and MeOP *N*-oxygenation, contribution was distributed more equally between FMO3 (50 and about 30%, respectively) and two CYP isoforms.

The results of incubations of the five DOAs using pHLM pretreated with the CYP inhibitor ABT are summarized in Fig. 7. Formation of the nor metabolites was significantly reduced by 80% for DALT or DMT and by 90% for MeOP or methamphetamine in comparison to the formation in control incubations. There was no nor 3-BMC detectable after preincubation with ABT. Residual formation of 3-BMC hydroxylamine was also reduced by 90%, of methamphetamine hydroxylamine by 50%, of MeOP *N*-oxide by 30%, and of DALT *N*-oxide and DMT *N*-oxide by 10% in comparison to formation in control incubations, respectively.

4. Discussion

4.1. Identification of FMO substrates by heat inactivation or chemical inhibition

FMOs and CYPs are both known to catalyze *N*-oxygenation (Cashman and Zhang, 2006), while CYPs, but not FMOs, catalyze nor metabolite formation via *N*-dealkylation, too. Thermal inactivation was supposed to be a suitable approach for elucidating the FMO activity. In the absence of NADPH, FMO3 was thermally labile and about 60 - 80% of enzyme activity was lost after heat treatment (50 - 60°C) for as short as 1 min (Cashman, 2008). No details about the mechanism behind this observation were given by the authors. Amitriptyline, clozapine, diphenhydramine, imipramine, prothipendyl, and ranitidine were already described as substrates of FMO isoforms of different species (Krueger and Williams, 2005). In the present

study, out of 12 tested substrates, known for *N*-oxygenation and *N*-dealkylation of their tertiary amine group, 11 showed formation of nor metabolites and 10 of *N*-oxides after incubations with untreated pHLM. Only ranitidine was neither *N*-oxygenated nor *N*-demethylated under the chosen incubation conditions. Furthermore, data obtained by heat-treated pHLM incubations could not be used to determine the role of FMOs in the formation of *N*-oxides, because the nor metabolite formation was also reduced even though CYPs should catalyze this reaction. A possible explanation would be the sensitivity of both, FMOs and CYPs to the used heat treatment, although FMO should be more sensitive to thermal inactivation under similar conditions (Cashman, 2008). To verify these results, a second heat inactivation protocol was tested for selected drugs using milder conditions (45°C, 5 min) according to Taniguchi-Takizawa et al. (Taniguchi-Takizawa *et al.*, 2015). For further experiments, amitriptyline, clozapine, and imipramine were chosen as known substrates of FMO and zopiclone showing highest *N*-oxide formation rate in the pHLM incubations. Again, both metabolic reactions were reduced by a comparable extend and significantly in comparison to untreated pHLM concerning amitriptyline, clozapine, and zopiclone. The formation of the imipramine *N*-oxide was reduced to a greater extent than that of the nor metabolite. Incubations with recombinant FMO3 confirmed the assumption that FMO3 was not involved in the nor metabolite formation, which supported the conclusion that CYPs were also thermally unstable.

As heat inactivation did not allow assessing the FMO contribution to *N*-oxide formations, chemical inhibitors were used to get further information. The first strategy was the inactivation of microsomal CYPs using preincubations with ABT, a known mechanism-based, non-specific CYP inhibitor. Although non-specific, ABT showed different inhibitor potencies towards the CYP isoforms (Emoto *et al.*, 2003). The following CYP isoform-specific reactions were used to test for sufficient ABT inhibition: 4-hydroxylation of bupropion for CYP2B6, *N*-deethylation of amodiaquine for CYP2C8, 5-hydroxylation of omeprazole for CYP2C19, and *O*-demethylation of dextromethorphan for CYP2D6 (U.S.Department of Health and Human Services *et al.*, 2006). Incubations were conducted as described by Dinger et al. (Dinger *et al.*, 2014). The formation of 4-hydroxy bupropion, *N*-deethyl amodiaquine, 5-hydroxy omeprazole, and *O*-demethyl dextromethorphan in pHLM preincubated with ABT was compared with the formation in incubations with untreated pHLM. Formation of these metabolites was almost entirely suppressed after treatment with ABT (remained

formation between 0 and 6%). The almost complete disappearance of the nor metabolites of amitriptyline, clozapine, imipramine, and zopiclone was in line with these findings (Fig. 3a). As ABT did not inactivate FMOs (Mathews *et al.*, 1985), the remaining *N*-oxide formation should be catalyzed by FMOs. Results of incubations with recombinant FMO3 and ABT were in line with findings of Mathews *et al.* and allowed the conclusion that the zopiclone *N*-oxide was exclusively formed by CYPs. The unaffected imipramine *N*-oxide formation indicated the predominant role of FMOs in this reaction. For amitriptyline and clozapine *N*-oxygenation, FMOs and also CYPs seemed to be involved.

On the other hand, FMO inactivation should be possible by methimazole (Hamman *et al.*, 2000). However, not only the formation of the *N*-oxides but also of the nor metabolites was significantly reduced. Hence, methimazole seemed to inhibit CYPs as well. These findings are in line with Guo et al. (Guo *et al.*, 1997), who already described methimazole as CYP inhibitor, but are in contrast to Taniguchi-Takizawa et al., who reported that methimazole had only little influence on the benzydamine *N*-demethylation (Taniguchi-Takizawa *et al.*, 2015). This again underlined the inconsistency in protocols concerning FMO3 incubation. However, as heat inactivation and chemical inhibition protocols were initially intended to identify FMO substrates and as the results obtained by both methods were not unambiguous, single enzyme incubations were finally chosen to identify enzymes involved in the *N*-oxygenation of the selected DOAs.

4.2. Identification of enzymes involved in the N-oxygenation

The aim was to identify all involved enzymes in the *N*-oxygenation of four therapeutic drugs and eights DOAs. Therefore, the established CYP initial activity screening approach (Caspar *et al.*, 2015; Meyer *et al.*, 2013c; Meyer *et al.*, 2014) was extended for FMO3. Five functional forms of FMO in humans are known with controversial data concerning their role in drug metabolism. In 2006, Cashman and Zhang identified FMO5 as most abundant FMO in the adult liver (Cashman and Zhang, 2006), followed by FMO3 and very little amounts of FMO1, 2, and 4. Other authors described FMO3 as major isoform, including the most recent work by Chen et al. (Cashman, 1995; Chen *et al.*, 2016; Overby *et al.*, 1997). However, FMO5 is

distinctly different from the other isoforms and does not catalyze the oxygenation of common FMO substrates (Cashman and Zhang, 2006). Hence, FMO3 represents the major enzyme involved in the human hepatic FMO-catalyzed metabolism and was therefore selected for further in vitro studies. For identification of the monooxygenases catalyzing the initial metabolic steps, FMO3 and the ten major human hepatic CYPs (Strolin *et al.*, 2007) were incubated under conditions allowing a statement on the qualitative involvement of a particular enzyme. Incubations with pHLM were conducted as positive control. All expected *N*-oxygenation products could be detected, except for methamphetamine, probably due to methamphetamine hydroxylamine levels below the detection limit.

Again, the monooxygenases activity screening showed zopiclone to be no substrate of FMO3. This further underlined the assumption that heat treatment and preincubation with methimazole had a negative influence on the activity of CYPs. Findings were also in line with the ABT inhibition results, where metabolite formation was almost totally reduced after ABT preincubation.

The amount of amitriptyline and imipramine *N*-oxide formed by FMO3 was very low. Both drugs were already described as substrates of FMO1 (Krueger and Williams, 2005; Phillips and Shephard, 2008). The small formation rates were in accordance to findings by Lemoine et al. They reported that human kidney preparations but not HLM catalyzed the *N*-oxygenation of imipramine and assumed the existence of different FMO isoforms (Lemoine *et al.*, 1990), while more recent works identified FMO1 as most prevalent FMO in the adult kidney (Cashman and Zhang, 2006). The detection of small amounts of the imipramine *N*-oxide in incubations with FMO3 in the present work might be due to more sensitive detection methods. Nevertheless, imipramine *N*-oxide formation was not negatively affected by treatment of pHLM with ABT in contrast to nor metabolite formation, even if the *N*-oxide was not exclusively formed by FMO3. Maybe the FMO activity increased after inhibition of CYPs. Not only imipramine, but also amitriptyline could be identified as FMO3 substrate. Breyer-Pfaff and Bull et al. described amitriptyline and imipramine as substrates of non-human FMOs (Breyer-Pfaff, 2004; Bull *et al.*, 1999), while Venkatakrishnan et al. referred to amitriptyline *N*-oxygenation as minor pathway in humans (Venkatakrishnan *et al.*, 2001). As the current results of the monooxygenases activity screening showed, the *N*-oxides of amitriptyline and clozapine were formed by FMO3

and CYPs, which confirmed the decreased formation after pretreatment of pHLM with ABT. For clozapine, the obtained results were in line with previous findings (Wang *et al.*, 2015).

Furthermore, eight DOAs were investigated using the monooxygenases activity screening. These DOAs were chosen because of their different chemical structures containing amine groups (see Fig. 1) and/or their known metabolic *N*-oxygenation (Cashman *et al.*, 1999; Meyer *et al.*, 2013b; Meyer *et al.*, 2015; Meyer *et al.*, 2012; Michely *et al.*, 2015; Riba *et al.*, 2012). Methamphetamine was already identified as substrate of human FMO3 (Cashman *et al.*, 1999). 3-BMC, DALT, dextromethorphan, DMT, glaucine, MeOP, and methadone have not been tested for *N*-oxygenation by FMO3. The *N*-oxide formation of dextromethorphan, glaucine, and methadone was not catalyzed by human FMO3 most probably due to sterical hindrance. Methamphetamine, 3-BMC, DALT, DMT, and MeOP were identified to be FMO3 substrates. However, *N*-oxygenation was not exclusively catalyzed by FMO3, but also by different CYP isoforms.

4.3. Kinetic studies, calculation of contributions, and hepatic clearances using a modified RAF approach

Chen et al. described the mean protein amount of FMO3 to be 46 pmol/mg in HLM (Chen *et al.*, 2016), which corresponded to CYP1A2 levels (42 pmol/mg HLM protein) (Shimada *et al.*, 1994). The RAF approach was described as tool to transfer recombinant enzyme kinetic data to human liver activity (Stormer *et al.*, 2000). Activity data provided by the manufacturer were used to calculate the RAF within this study (Stormer *et al.*, 2000).

The two therapeutic drugs amitriptyline and clozapine and their corresponding *N*-oxides were used to compare the hepatic net clearances calculated via CRS or PAR. As already described by Meyer et al., missing analytical standards for absolute quantification of formed metabolites might be a bottleneck in the assessment of kinetic data (Meyer *et al.*, 2013a). The use of simple PAR of formed metabolite and internal standard was an alternative to calculate the contribution of enzymes to the hepatic clearance (Meyer *et al.*, 2013a). As shown in Table 2, there was no significant difference in contributions calculated via CRS and PAR for amitriptyline

and clozapine. Hence, relative V_{max} values were a useful tool for comparison of velocities of different enzymes catalyzing the same reaction and for assessing their contributions to the hepatic clearance. In conclusion, neither CRS nor PAR had substantial impact on the estimation of in vivo hepatic net clearance. This was in line with previous findings (Meyer *et al.*, 2013a).

Results for amitriptyline and clozapine indicated that FMO3 only played a minor role in their hepatic clearance as only 1 - 8% of amitriptyline and clozapine were excreted as *N*-oxide (Santagostino *et al.*, 1974; Schaber *et al.*, 1998). However, as the amitriptyline *N*-oxide was formed immediately after administration and disappeared soon, the *N*-oxygenation was discussed as 'emergency' route of metabolism for high drug levels (Santagostino *et al.*, 1974). This assumption was consistent with the findings presented here of high FMO3 K_m and V_{max} values, indicating a fast metabolism of high drug levels.

N-Oxygenation after CYP inhibition in pHLM was about 20% and thus higher than expected. Possible explanations were that either FMO3 worked more efficiently if CYPs were inhibited or the involved CYPs were not completely inhibited by ABT. However, these results confirmed the low contribution of FMO3 calculated via the RAF approach. RAF calculations were also done for different substrate concentrations (0.1 - 25 µM) to cover different concentration ranges but only minor changes in calculated in vivo enzyme contributions were observed. Dextromethorphan, glaucine, and methadone were not metabolized by FMO3 and no further investigations were conducted, as the hepatic clearance of their *N*-oxides was expected to be only CYP-mediated.

Concerning the five DOAs identified as FMO3 substrates, only PAR could be used for calculating in vivo contribution. 3-BMC hydroxylamine was predominantly formed by CYP isoforms, while the formation of all other *N*-oxides was mainly FMO3-dependent. In order to confirm these calculations, pHLM incubations after ABT inhibition were performed and nor metabolites were monitored to verify successful CYP inhibition. 3-BMC hydroxylamine formation was significantly reduced after CYP inhibition but *N*-oxygenation of the other DOAs was not influenced by ABT inhibition and remained at more than 50% of formation in control incubations. These data fitted well with the higher contributions of FMO3 calculated using the RAF approach. FMO3 contribution did not change with increasing substrate concentrations

calculated based on reported DMT and methamphetamine plasma concentrations (Huestis and Cone, 2007; Oliveira *et al.*, 2012).

As FMO3 and different CYP isoforms (one in case of DALT and methamphetamine, two for DMT and MeOP, up to five for 3-BMC) were involved in the hepatic clearance of the *N*-oxygenation products of all investigated DOAs, a clinically relevant interaction with single inhibitors should not be expected. In addition, further metabolic steps were described to contribute to the total hepatic clearance (Cashman *et al.*, 1999; Meyer *et al.*, 2013b; Meyer *et al.*, 2015; Meyer *et al.*, 2012; Michely *et al.*, 2015; Riba *et al.*, 2012). Finally, FMO3 was not expected to be induced or inhibited by other substances (Cashman and Zhang, 2006) as described for CYPs.

5. Conclusions

Only single enzyme incubations were suitable for unambiguous identification of FMO3 substrates as heat inactivation and chemical inhibition provided contradictory results. Kinetic parameters of the *N*-oxygenation reactions were determined using the involved, recombinant enzymes. Finally, FMO3 was included for the first time in the RAF approach and its contribution to the human, hepatic clearance could be calculated. FMO3 was identified as enzyme mainly responsible for the formation of *N,N*-diallyltryptamine *N*-oxide and methamphetamine hydroxylamine (> 80% contribution for both). A contribution of 50 and 30% was calculated for the formation of *N,N*-dimethyltryptamine *N*-oxide and methoxypiperamide *N*-oxide, respectively. However, FMO3 contributed with less than 5% to the formation of 3-bromomethcathinone hydroxylamine, amitriptyline *N*-oxide, and clozapine *N*-oxide. There was no significant difference in the contributions when using calibrations with reference metabolite standards or peak area ratio calculations. As the application of the RAF approach containing FMO3 was not described in literature so far, the importance of FMO3 in the *N*-oxygenation of DOAs in human metabolism was shown for the first time here.

Conflict of interest

The authors declared no conflict of interest.

Acknowledgements

The authors like to thank Achim T. Caspar, Julia Dinger, Andreas G. Helfer, Julian A. Michely, Lilian H.J. Richter, and Armin A. Weber for their support and fruitful discussion.

References

Breyer-Pfaff, U., 2004. The metabolic fate of amitriptyline, nortriptyline and amitriptylinoxide in man. Drug Metab Rev. 36, 723-746.

Bull, S., Catalani, P., Garle, M., Coecke, S., Clothier, R., 1999. Imipramine for Cytochrome P450 Activity Determination: a Multiple-species Metabolic Probe. Toxicol. In Vitro 13, 537-541.

Cashman, J.R., 1995. Structural and catalytic properties of the mammalian flavin-containing monooxygenase. Chem. Res. Toxicol. 8, 166-181.

Cashman, J.R., 2005. Some distinctions between flavin-containing and cytochrome P450 monooxygenases. Biochem. Biophys. Res. Commun. 338, 599-604.

Cashman, J.R., 2008. Role of flavin-containing monooxygenase in drug development. Expert. Opin. Drug Metab Toxicol. 4, 1507-1521.

Cashman, J.R., Xiong, Y.N., Xu, L., Janowsky, A., 1999. N-oxygenation of amphetamine and methamphetamine by the human flavin-containing monooxygenase (form 3): role in bioactivation and detoxication. J. Pharmacol. Exp. Ther. 288, 1251-1260.

Cashman, J.R. Zhang, J., 2006. Human flavin-containing monooxygenases. Annu. Rev. Pharmacol. Toxicol. 46, 65-100.

Caspar, A.T., Helfer, A.G., Michely, J.A., Auwaerter, V., Brandt, S.D., Meyer, M.R., Maurer, H.H., 2015. Studies on the metabolism and toxicological detection of the new psychoactive designer drug 2-(4-iodo-2,5-dimethoxyphenyl)-N-[(2-methoxyphenyl)methyl]ethanamine (25I-NBOMe) in human and rat urine using GC-MS, LC-MSn, and LC-HR-MS/MS. Anal. Bioanal. Chem. 407, 6697-6719.

Chauret, N., Gauthier, A., Nicoll-Griffith, D.A., 1998. Effect of Common Organic Solvents on in Vitro Cytochrome P450-Mediated Metabolic Activities in Human Liver Microsomes. Drug Metab. Dispos. 26, 1-4.

Chen, Y., Zane, N.R., Thakker, D.R., Wang, M.Z., 2016. Quantification of Flavin-containing Monooxygenases 1, 3 and 5 in Human Liver Microsomes by UPLC-MRM-based

Targeted Quantitative Proteomics and Its Application to the Study of Ontogeny. Drug Metab Dispos. [Epub ahead of print].

Crespi, C.L. Miller, V.P., 1999. The use of heterologously expressed drug metabolizing enzymes-state of the art and prospects for the future. Pharmacol. Ther. 84, 121-131.

Cruciani, G., Valeri, A., Goracci, L., Pellegrino, R.M., Buonerba, F., Baroni, M., 2014. Flavin monooxygenase metabolism: why medicinal chemists should matter. J. Med. Chem. 57, 6183-6196.

Dinger, J., Meyer, M.R., Maurer, H.H., 2014. Development of an in vitro cytochrome P450 cocktail inhibition assay for assessing the inhibition risk of drugs of abuse. Toxicol. Lett. 230, 28-35.

Emoto, C., Murase, S., Sawada, Y., Jones, B.C., Iwasaki, K., 2003. In vitro inhibitory effect of 1-aminobenzotriazole on drug oxidations catalyzed by human cytochrome P450 enzymes: a comparison with SKF-525A and ketoconazole. Drug Metab Pharmacokinet. 18, 287-295.

Fan, P.W., Zhang, D., Driscoll, J.P., Halladay, J.S., Khojasteh, C., 2016. Going beyond common drug metabolizing enzymes: Case studies of biotransformation involving aldehyde oxidase, gamma-glutamyl transpeptidase, cathepsin B, flavin-containing monooxygenase, and ADP-ribosyltransferase. Drug Metab. Dispos. [Epub ahead of print].

Guo, Z., Raeissi, S., White, R.B., Stevens, J.C., 1997. Orphenadrine and methimazole inhibit multiple cytochrome P450 enzymes in human liver microsomes. Drug Metab. Dispos. 25, 390-393.

Hamman, M.A., Haehner-Daniels, B.D., Wrighton, S.A., Rettie, A.E., Hall, S.D., 2000. Stereoselective sulfoxidation of sulindac sulfide by flavin-containing monooxygenases. Comparison of human liver and kidney microsomes and mammalian enzymes. Biochem. Pharmacol. 60, 7-17.

Huestis, M.A. Cone, E.J., 2007. Methamphetamine disposition in oral fluid, plasma, and urine. Ann. N. Y. Acad. Sci. 1098, 104-121.

Krueger, S.K. Williams, D.E., 2005. Mammalian flavin-containing monooxygenases: structure/function, genetic polymorphisms and role in drug metabolism. Pharmacol. Ther. 106, 357-387.

Lemoine, A., Johann, M., Cresteil, T., 1990. Evidence for the presence of distinct flavin-containing monooxygenases in human tissues. Arch. Biochem. Biophys. 276, 336-342.

Mathews, J.M., Dostal, L.A., Bend, J.R., 1985. Inactivation of rabbit pulmonary cytochrome P-450 in microsomes and isolated perfused lungs by the suicide substrate 1-aminobenzotriazole. J. Pharmacol. Exp. Ther. 235, 186-190.

Meyer, G.M.J., Meyer, M.R., Wink, C.S.D., Zapp, J., Maurer, H.H., 2013a. Studies on the in vivo contribution of human cytochrome P450s to the hepatic metabolism of glaucine, a new drug of abuse. Biochem. Pharmacol. 86, 1497-1506.

Meyer, G.M.J., Meyer, M.R., Wissenbach, D.K., Maurer, H.H., 2013b. Studies on the metabolism and toxicological detection of glaucine, an isoquinoline alkaloid from *Glaucium flavum* (Papaveraceae), in rat urine using GC-MS, LC-MS^n and LC-high-resolution MS^n. J. Mass Spectrom. 48, 24-41.

Meyer, M.R., Bach, M., Welter, J., Bovens, M., Turcant, A., Maurer, H.H., 2013c. Ketamine-derived designer drug methoxetamine: metabolism including isoenzyme kinetics and toxicological detectability using GC-MS and LC-(HR-)MSn. Anal. Bioanal. Chem. 405, 6307-6321.

Meyer, M.R., Holderbaum, A., Kavanagh, P., Maurer, H.H., 2015. Low and high resolution MS for studies on the metabolism and toxicological detection of the new psychoactive substance methoxypiperamide (MeOP). J. Mass Spectrom. 50, 1163-1174.

Meyer, M.R., Lindauer, C., Welter, J., Maurer, H.H., 2014. Dimethocaine, a synthetic cocaine derivative: Studies on its in vivo metabolism and its detectability in urine by LC-HR-MS^n and GC-MS using a rat model. Anal. Bioanal. Chem. 406, 1845-1854.

Meyer, M.R., Vollmar, C., Schwaninger, A.E., Maurer, H.H., 2012. New cathinone-derived designer drugs 3-bromomethcathinone and 3-fluoromethcathinone: studies on their

metabolism in rat urine and human liver microsomes using GC-MS and LC-high-resolution MS and their detectability in urine. J. Mass Spectrom. 47, 253-262.

Michely, J.A., Helfer, A.G., Brandt, S.D., Meyer, M.R., Maurer, H.H., 2015. Metabolism of the new psychoactive substances N,N-diallyltryptamine (DALT) and 5-methoxy-DALT and their detectability in urine by GC-MS, LC-MSn, and LC-HR-MS/MS. Anal Bioanal. Chem. 407, 7831-7842.

Oliveira, C.D., Okai, G.G., da Costa, J.L., de Almeida, R.M., Oliveira-Silva, D., Yonamine, M., 2012. Determination of dimethyltryptamine and beta-carbolines (ayahuasca alkaloids) in plasma samples by LC-MS/MS. Bioanalysis. 4, 1731-1738.

Overby, L.H., Carver, G.C., Philpot, R.M., 1997. Quantitation and kinetic properties of hepatic microsomal and recombinant flavin-containing monooxygenases 3 and 5 from humans. Chem. Biol. Interact. 106, 29-45.

Phillips, I.R. Shephard, E.A., 2008. Flavin-containing monooxygenases: mutations, disease and drug response. Trends Pharmacol. Sci. 29, 294-301.

Riba, J., McIlhenny, E.H., Valle, M., Bouso, J.C., Barker, S.A., 2012. Metabolism and disposition of N,N-dimethyltryptamine and harmala alkaloids after oral administration of ayahuasca. Drug Test. Anal. 4, 610-616.

Ring, B.J., Wrighton, S.A., Aldridge, S.L., Hansen, K., Haehner, B., Shipley, L.A., 1999. Flavin-containing monooxygenase-mediated N-oxidation of the M(1)-muscarinic agonist xanomeline. Drug Metab Dispos. 27, 1099-1103.

Santagostino, G., Facino, R.M., Pirillo, D., 1974. Urinary excretion of amitriptyline N-oxide in humans. J. Pharm. Sci. 63, 1690-1692.

Schaber, G., Stevens, I., Gaertner, H.J., Dietz, K., Breyer-Pfaff, U., 1998. Pharmacokinetics of clozapine and its metabolites in psychiatric patients: plasma protein binding and renal clearance. Br. J. Clin. Pharmacol. 46, 453-459.

Shimada, T., Yamazaki, H., Mimura, M., Inui, Y., Guengerich, F.P., 1994. Interindividual variations in human liver cytochrome P-450 enzymes involved in the oxidation of

drugs, carcinogens and toxic chemicals: studies with liver microsomes of 30 Japanese and 30 Caucasians. J. Pharmacol. Exp. Ther. 270, 414-423.

Stormer, E., von Moltke, L.L., Greenblatt, D.J., 2000. Scaling drug biotransformation data from cDNA-expressed cytochrome P-450 to human liver: a comparison of relative activity factors and human liver abundance in studies of mirtazapine metabolism. J. Pharmacol. Exp. Ther. 295, 793-801.

Strolin, B.M., Tipton, K.F., Whomsley, R., 2007. Amine oxidases and monooxygenases in the in vivo metabolism of xenobiotic amines in humans: has the involvement of amine oxidases been neglected? Fundam. Clin. Pharmacol. 21, 467-480.

Strolin, B.M., Whomsley, R., Baltes, E., 2006. Involvement of enzymes other than CYPs in the oxidative metabolism of xenobiotics. Expert. Opin. Drug Metab Toxicol. 2, 895-921.

Szoko, E., Tabi, T., Borbas, T., Dalmadi, B., Tihanyi, K., Magyar, K., 2004. Assessment of the N-oxidation of deprenyl, methamphetamine, and amphetamine enantiomers by chiral capillary electrophoresis: an in vitro metabolism study. Electrophoresis 25, 2866-2875.

Taniguchi-Takizawa, T., Shimizu, M., Kume, T., Yamazaki, H., 2015. Benzydamine N-oxygenation as an index for flavin-containing monooxygenase activity and benzydamine N-demethylation by cytochrome P450 enzymes in liver microsomes from rats, dogs, monkeys, and humans. Drug Metab Pharmacokinet. 30, 64-69.

Torres Pazmino, D.E., Winkler, M., Glieder, A., Fraaije, M.W., 2010. Monooxygenases as biocatalysts: Classification, mechanistic aspects and biotechnological applications. J. Biotechnol. 146, 9-24.

U.S.Department of Health and Human Services, Food and Drug Administration, Center for Drug Evaluation and Research (CDER), Center for Biologics Evaluation and Research (CBER) Guidance for Industry: Drug Interaction Studies - Study Design, Data Analysis, and Implications for Dosing and Labeling [Draft]. http://www.fda.gov/downloads/drugs/guidancecomplianceregulatoryinformation/guidances/ucm292362.pdf

Venkatakrishnan, K., von Moltke, L.L., Greenblatt, D.J., 2001. Application of the relative activity factor approach in scaling from heterologously expressed cytochromes p450 to human liver microsomes: studies on amitriptyline as a model substrate. J. Pharmacol. Exp. Ther. 297, 326-337.

Wang, W., Tian, D.D., Zheng, B., Wang, D., Tan, Q.R., Wang, C.Y., Zhang, Z.J., 2015. Peony-Glycyrrhiza Decoction, an Herbal Preparation, Inhibits Clozapine Metabolism via Cytochrome P450s, but Not Flavin-Containing Monooxygenase in In Vitro Models. Drug Metab Dispos. 43, 1147-1153.

Wissenbach, D.K., Meyer, M.R., Remane, D., Philipp, A.A., Weber, A.A., Maurer, H.H., 2011a. Drugs of abuse screening in urine as part of a metabolite-based LC-MS(n) screening concept. Anal. Bioanal. Chem. 400, 3481-3489.

Wissenbach, D.K., Meyer, M.R., Remane, D., Weber, A.A., Maurer, H.H., 2011b. Development of the first metabolite-based LC-MSn urine drug screening procedure - exemplified for antidepressants. Anal. Bioanal. Chem. 400, 79-88.

Zollner, A., Buchheit, D., Meyer, M.R., Maurer, H.H., Peters, F.T., Bureik, M., 2010. Production of human phase 1 and 2 metabolites by whole-cell biotransformation with recombinant microbes. Bioanalysis 2, 1277-1290.

Table 1 Determined Michaelis-Menten values (percentage errors in brackets) for each formed metabolite by corresponding enzymes (FMO3, pHLM, CYPs), calculated using corresponding reference standards (CRS) or peak area ratios (PAR). All K_m values were given in μM, V_{max} (CRS) in pmol/min/mg and V_{max} (PAR) in AU/min/mg. ND: not determined due to insufficient activity

Formed metabolite	Determined via	Michaelis-Menten values, K_m / V_{max}								
		FMO3	**pHLM**	**CYP1A2**	**CYP2B6**	**CYP2C8**	**CYP2C19**	**CYP2D6**	**CYP2E1**	**CYP3A4**
Amitriptyline *N*-oxide	CRS	1689 (20) / 1323 (14)	90 (13) / 28 (4)	125 (13) / 149 (6)	9.3 (37) / 60 (13)	ND	6.0 (20) / 68 (4)	15 (15) / 181 (4)	ND	ND
Amitriptyline *N*-oxide	PAR	1671 (20) / 20 (14)	86 (13) / 0.43 (4)	115 (13) / 2.3 (6)	8.9 (36) / 0.93 (13)	ND	6.4 (27) / 1.2 (5)	14 (15) / 2.8 (4)	ND	ND
Clozapine *N*-oxide	CRS	147 (13) / 790 (4)	11 (23) / 49 (6)	9.5 (17) / 54 (5)	ND	7.2 (19) / 25 (6)	3.1 (32) / 244 (10)	22 (15) / 14 (5)	ND	10 (14) / 1341 (4)
Clozapine *N*-oxide	PAR	147 (13) / 2.0 (4)	11 (24) / 0.13 (6)	9.6 (18) / 0.14 (5)	ND	7.0 (19) / 0.02 (5)	3.2 (31) / 0.17 (12)	21 (18) / 0.01 (5)	ND	11 (15) / 1.0 (4)
3-BMC hydroxylamine	PAR	3022 (8) / 12 (5)	893 (11) / 0.62 (5)	2927 (11) / 7.0 (7)	165 (11) / 1.1 (3)	ND	229 (10) / 4.2 (3)	ND	1498 (7) / 3.8 (4)	552 (11) / 1.8 (4)
DALT *N*-oxide	PAR	355 (14) / 34 (6)	300 (18) / 0.35 (7)	ND	ND	ND	ND	ND	ND	131 (26) / 0.23 (10)
DMT *N*-oxide	PAR	421 (7) / 164 (3)	307 (10) / 4.2 (4)	172 (9) / 9.7 (3)	ND	ND	107 (9) / 1.8 (3)	ND	ND	ND
MeOP *N*-oxide	PAR	671 (4) / 15 (2)	517 (9) / 1.0 (4)	ND	ND	ND	55 (8) / 2.9 (2)	ND	ND	717 (9) / 3.7 (5)
Methamphetamine hydroxylamine	PAR	13483 (29) / 15 (22)	ND	ND	ND	ND	ND	558 (20) / 0.12 (8)	ND	ND

Table 2 Calculated in vivo hepatic net clearance [%] of the *N*-oxygenation products for the used enzymes (FMO3, CYPs) at different substrate concentrations (0.1/1/10/25 µM), calculated using corresponding reference standards (CRS) or peak area ratios (PAR).

Formed metabolite	Determined via	Hepatic net clearance at a substrate concentration of 0.1 / 1 / 10 / 25 µM [%]							
		FMO3	**CYP1A2**	**CYP2B6**	**CYP2C8**	**CYP2C19**	**CYP2D6**	**CYP2E1**	**CYP3A4**
Amitriptyline *N*-oxide	CRS	1 / 1 / 2 / 2	25 / 27 / 37 / 47	36 / 35 / 28 / 22		9 / 8 / 5 / 4	29 / 29 / 28 / 25		
	PAR	1 / 1 / 2 / 2	25 / 27 / 37 / 48	36 / 35 / 28 / 22		9 / 8 / 5 / 4	29 / 29 / 28 / 24		
Clozapine *N*-oxide	CRS	1 / 1 / 1 / 2	5 / 5 / 5 / 5		5 / 5 / 5 / 4	3 / 2 / 1 / 1	<1 / <1 / <1 / <1		86 / 87 / 88 / 88
	PAR	2 / 2 / 3 / 5	16 / 16 / 16 / 15		5 / 5 / 4 / 4	2 / 2 / 2 / 1	<1 / <1 / <1 / <1		75 / 75 / 75 / 75
3-BMC hydroxylamine	PAR	4 / 4 / 4 / 4	16 / 16 / 17 / 17	22 / 21 / 21 / 20		6 / 6 / 5 / 5		28 / 29 / 29 / 30	24 / 24 / 24 / 24
DALT *N*-oxide	PAR	90 / 90 / 91 / 91							10 / 10 / 9 / 9
DMT *N*-oxide	PAR	49 / 49 / 50 / 51	50 / 50 / 49 / 48			1 / 1 / 1 / 1			
MeOP *N*-oxide	PAR	32 / 32 / 33 / 34				24 / 24 / 21 / 18			44 / 44 / 46 / 48
Methamphetamine hydroxylamine	PAR	84 / 84 / 85 / 85					16 / 16 / 15 / 15		

Legends to the Figures

Fig. 1. Chemical structures of tested drugs of abuse in alphabetic order.

Fig. 2. Effect of heat treatment of pHLM (a: 55°C, 1 min; b: 45°C, 5 min) on the formation of *N*-oxide (open bars) and nor metabolite (shaded bars) of therapeutic drugs. Data represent formation rates relative to formation in control incubations with untreated pHLM. Values are expressed as mean and were tested for significance (n = 2; ***, $P < 0.001$ for formation in incubations with heat-treated pHLM versus formation in control incubations).

Fig. 3. Effect of preincubation with ABT (a) or methimazole (b) of pHLM on the formation of *N*-oxide (open bars) and nor metabolite (shaded bars) of four therapeutic drugs. Data represent formation rates relative to formation in control incubations with untreated pHLM. Values are expressed as mean and were tested for significance (n = 2; ***, $P < 0.001$ for formation in incubations with pHLM preincubated with ABT or methimazole versus formation in control incubations).

Fig. 4. Kinetics of FMO3, pHLM, and single CYP of the corresponding *N*-oxygenations calculated using corresponding reference standards (CRS) or peak area ratios (PAR). Data points represent means and ranges of triplicate incubations.

Fig. 5. Estimated in vivo hepatic net clearance of amitriptyline *N*-oxide calculated using corresponding reference standards (CRS) or peak area ratios (PAR) for different substrate concentrations.

Fig. 6. Estimated in vivo hepatic net clearance of the *N*-oxygenation products of clozapine and different drugs of abuse using PAR at a substrate concentration of 0.1 µM.

Fig. 7. Effect of ABT preincubation of pHLM on the formation of *N*-oxygenation products (open bars) and nor metabolites (shaded bars) of five drugs of abuse. Data represent formation rates relative to formation in control incubations with untreated pHLM. Data are expressed as mean and were tested for significance (n = 2; ***, $P < 0.001$ for formation in incubations with pHLM preincubated with ABT versus formation in control incubations).

Figure 1

Click here to download high resolution image

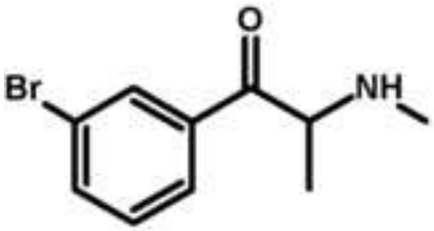

3-Bromomethcathinone

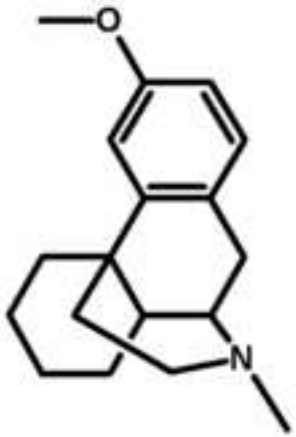

Dextromethorphan

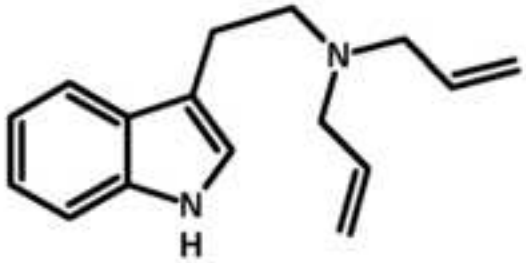

N,N-Diallyltryptamine

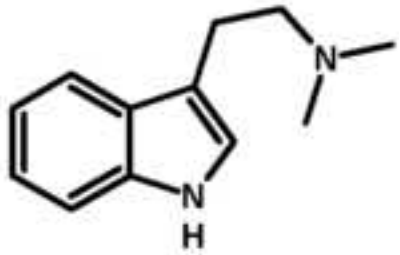

N,N-Dimethyltryptamine

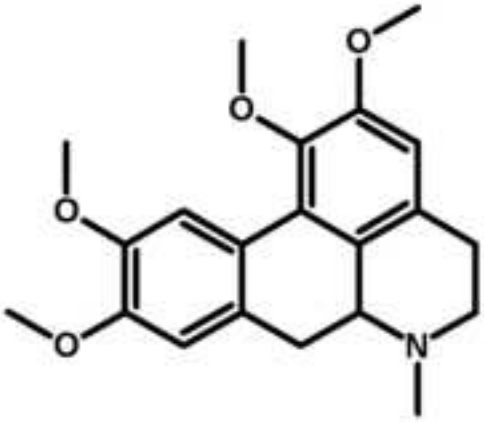

Glaucine

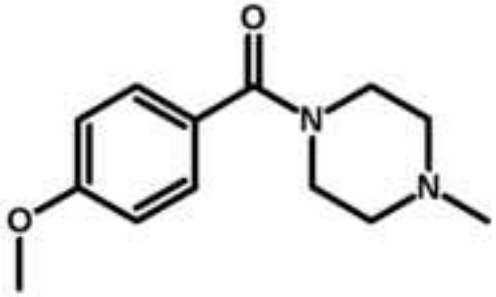

Methoxypiperamide

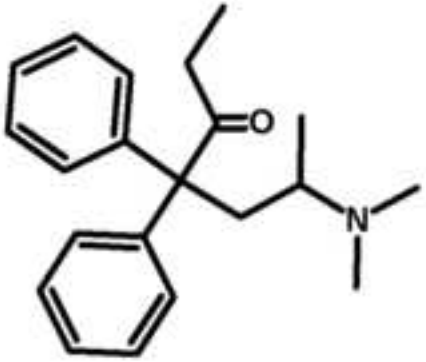

Methadone

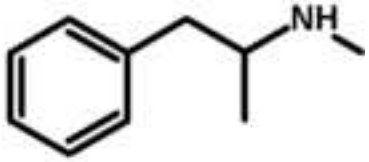

Methamphetamine

Figure 2a

Click here to download high resolution image

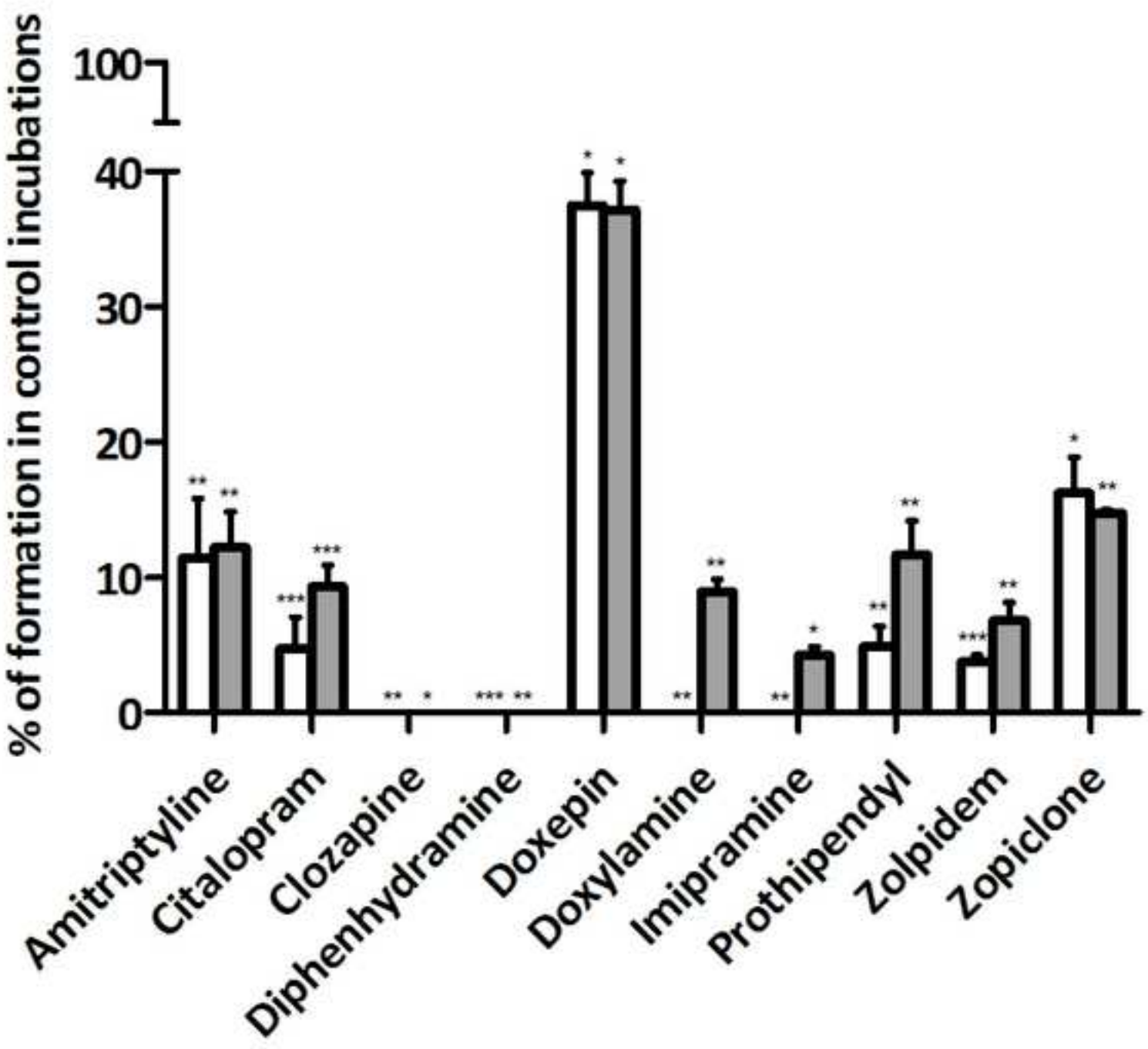

Figure 2b

Click here to download high resolution image

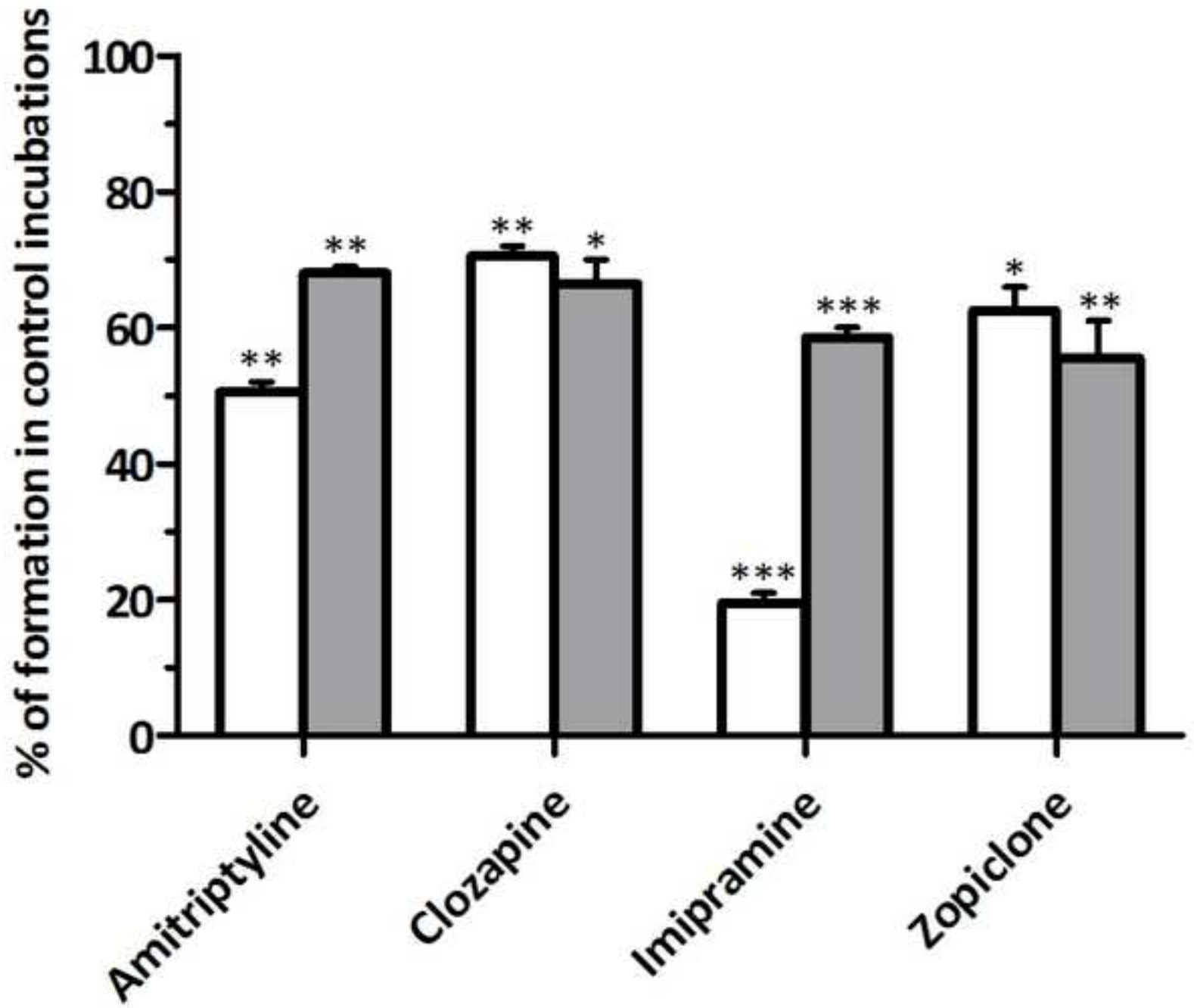

Figure 3a

Click here to download high resolution image

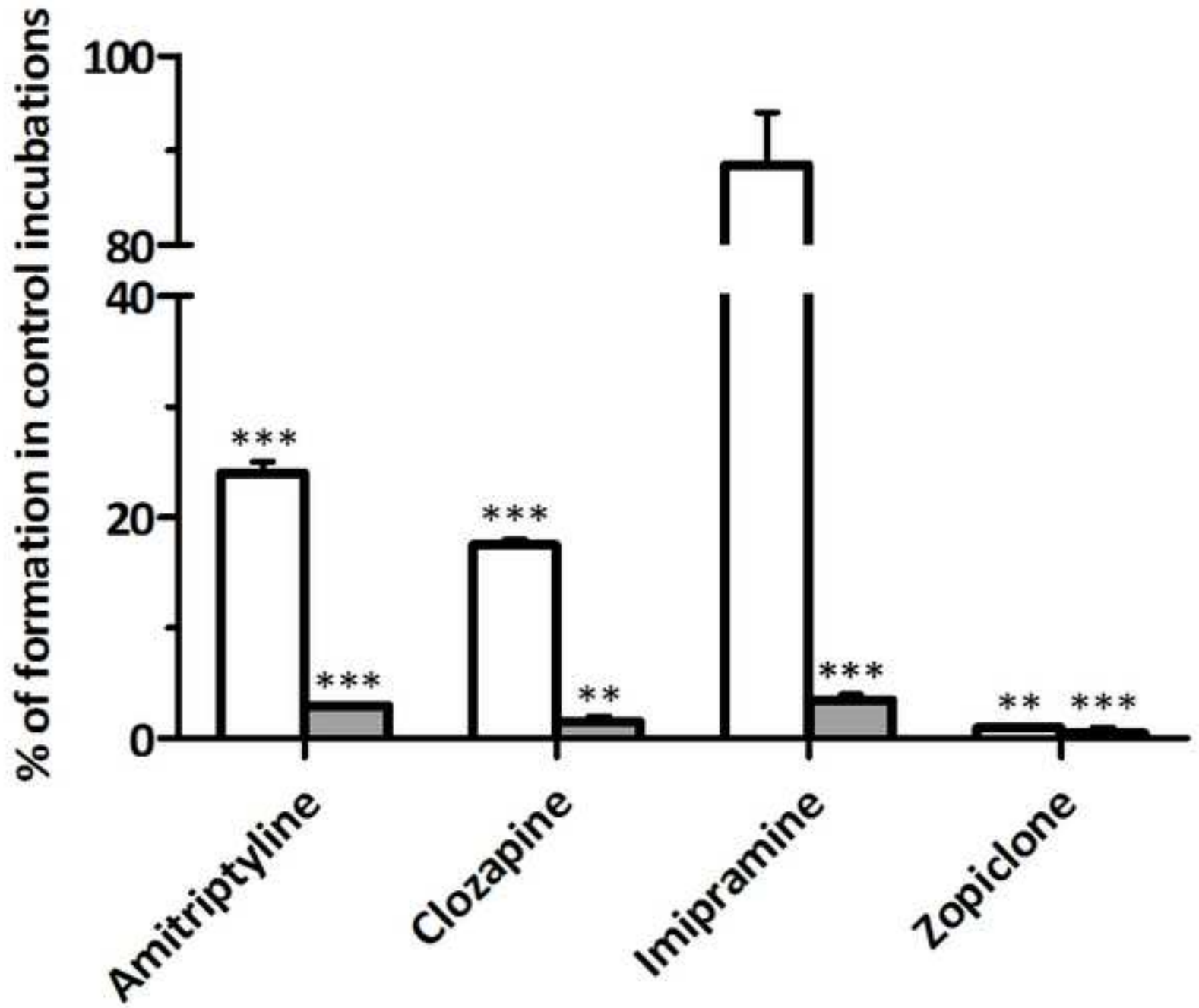

Figure 3b

Click here to download high resolution image

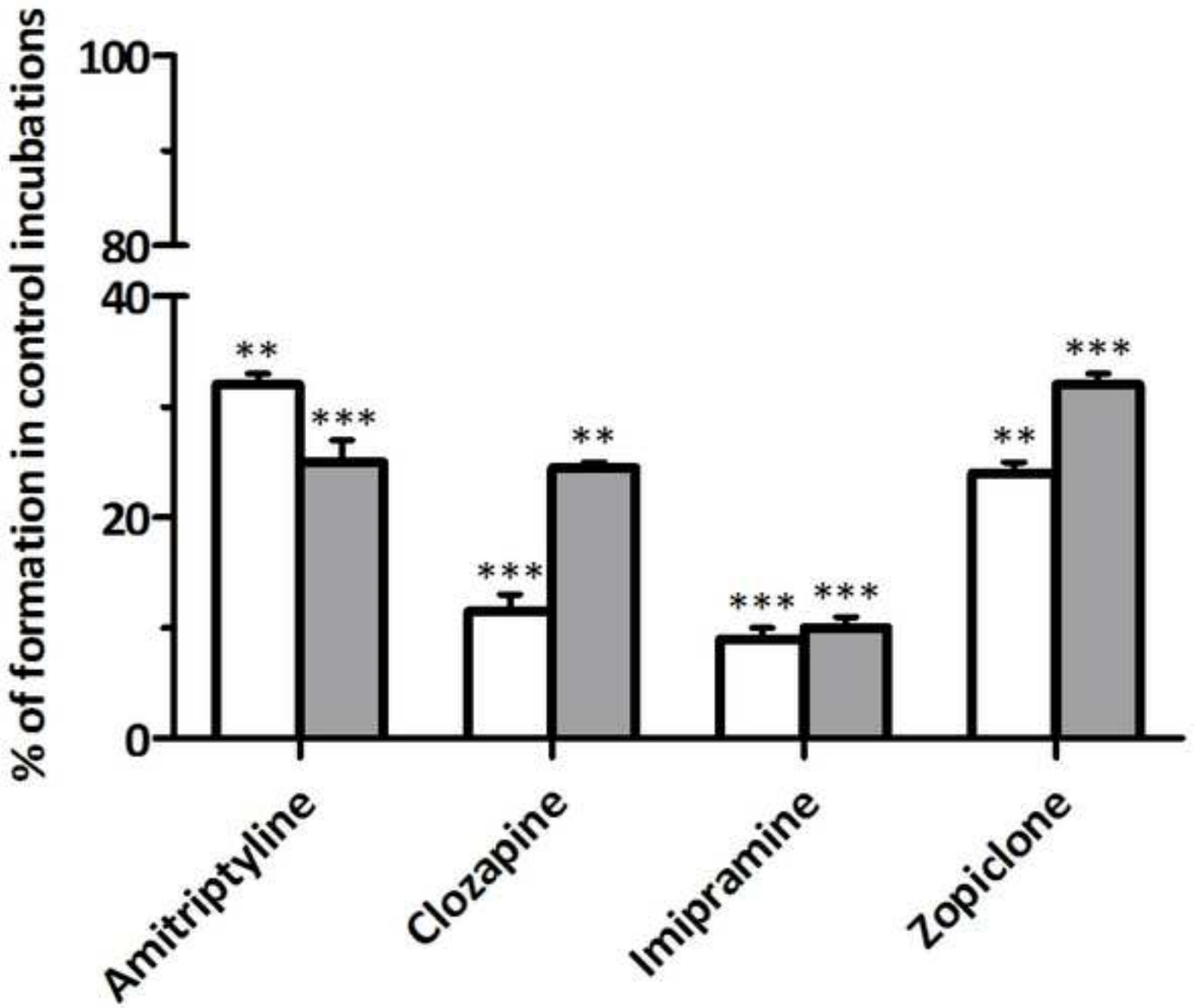

Figure 4

Click here to download high resolution image

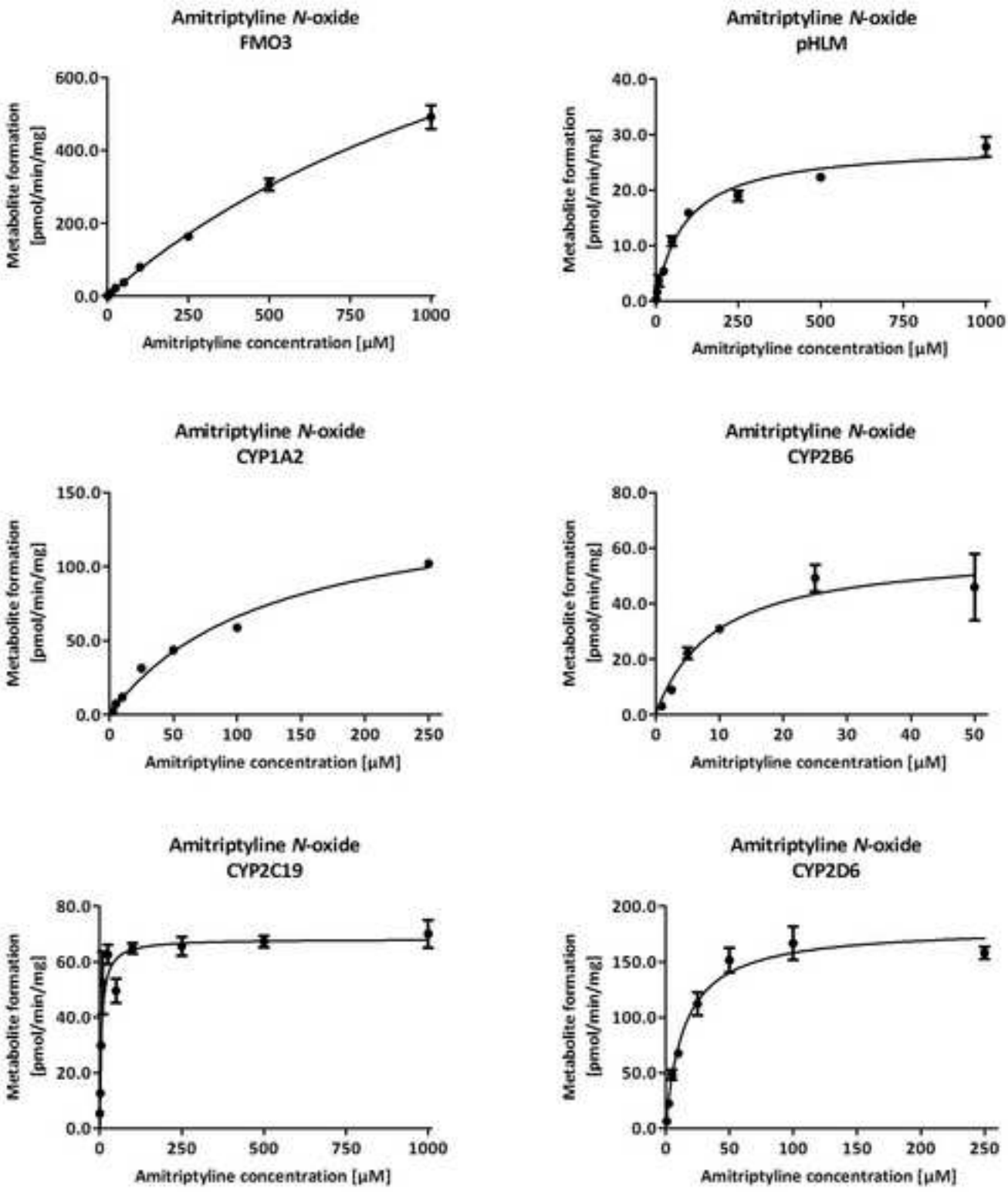

Figure 4

Click here to download high resolution image

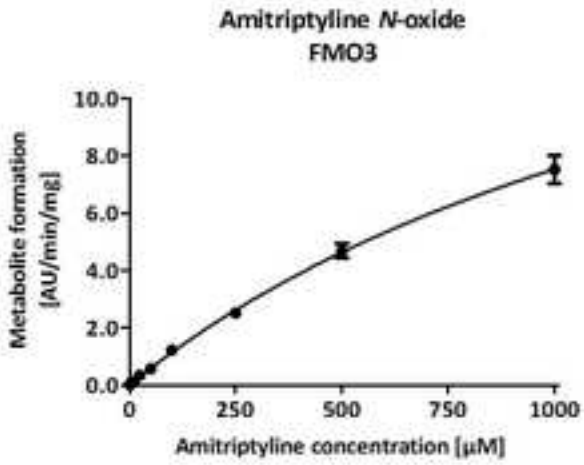

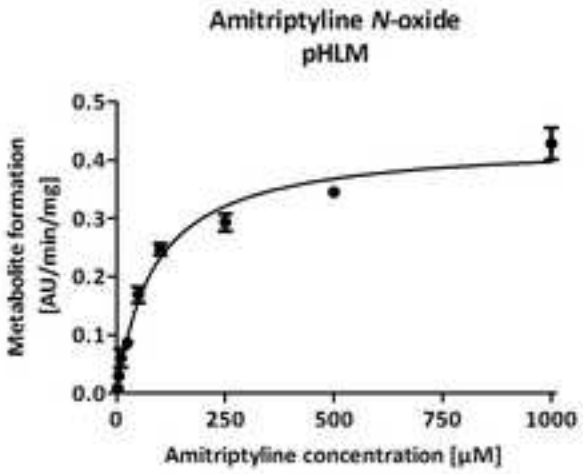

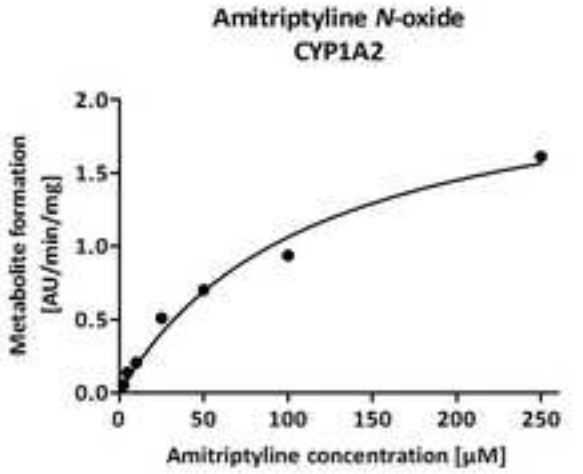

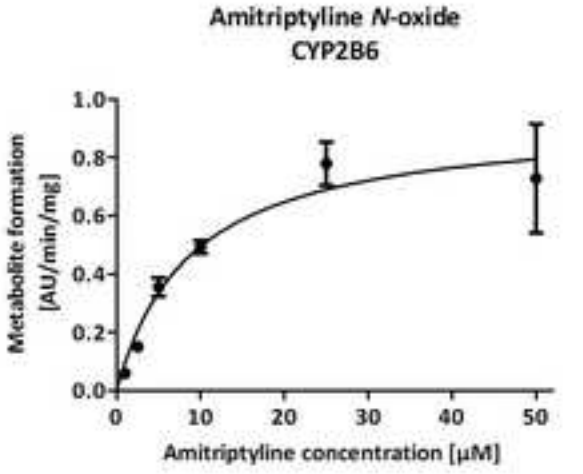

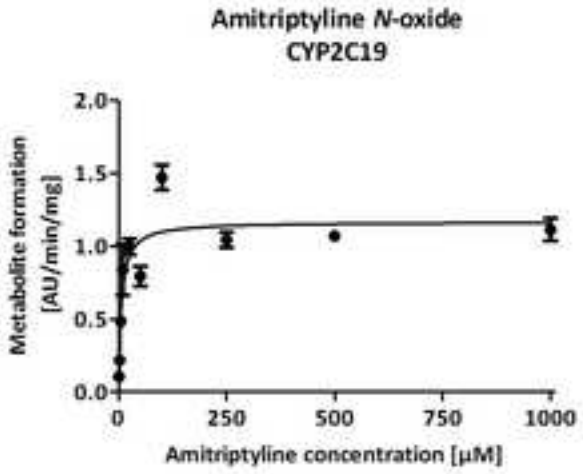

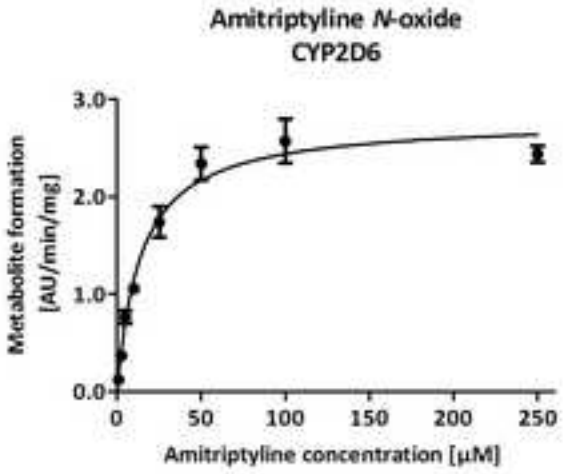

Figure 4

Click here to download high resolution image

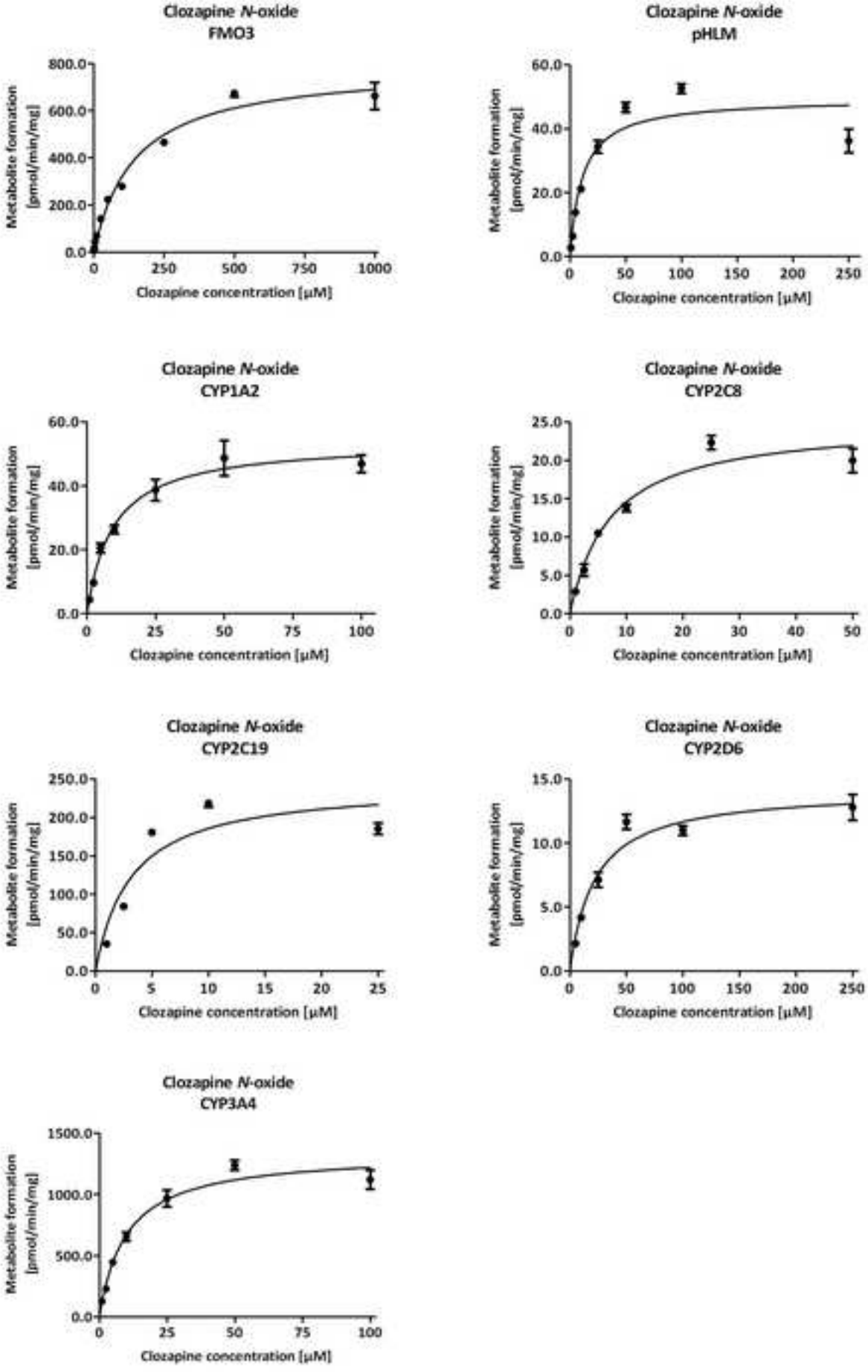

Figure 4

Click here to download high resolution image

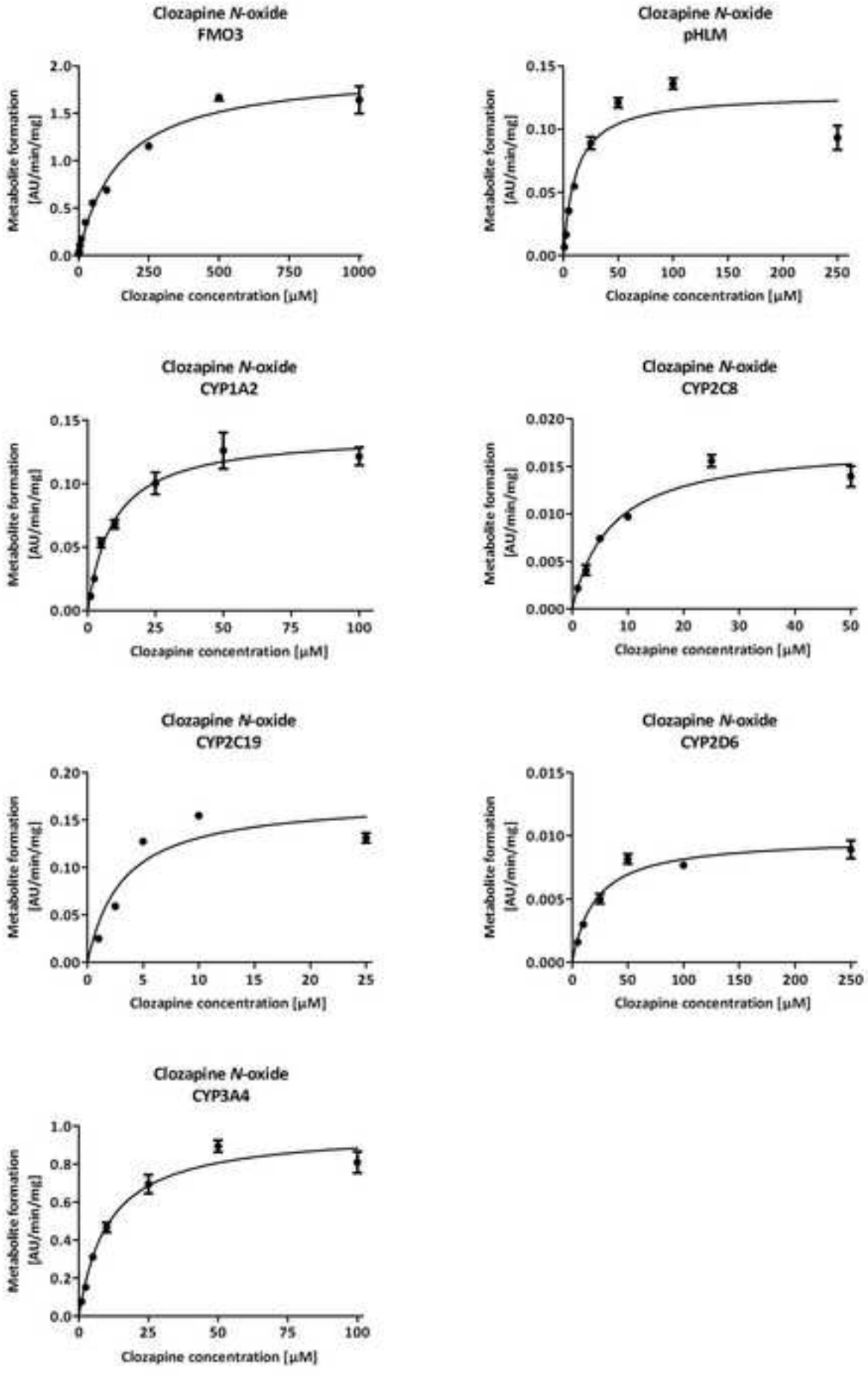

Figure 4

Click here to download high resolution image

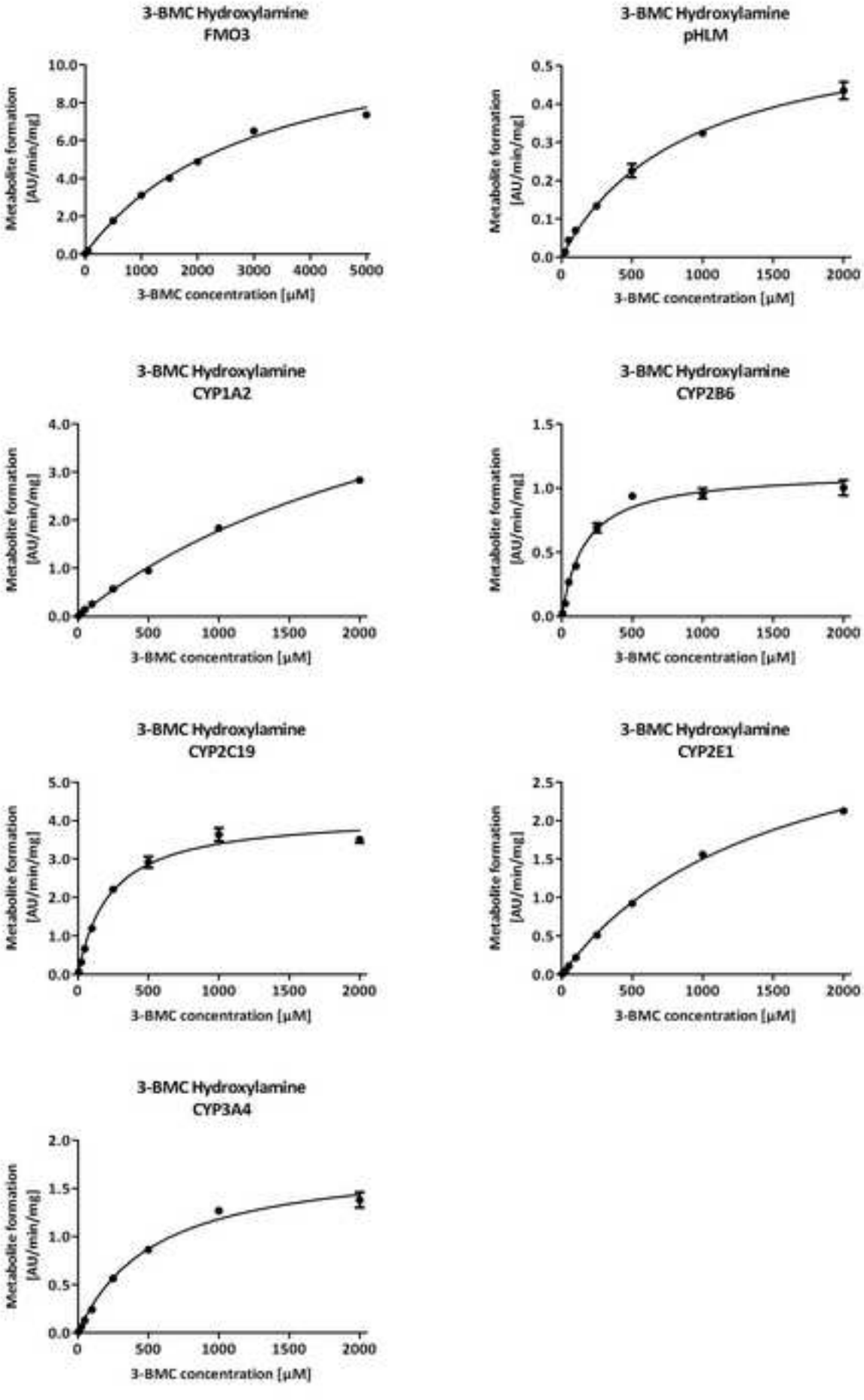

Figure 4

Click here to download high resolution image

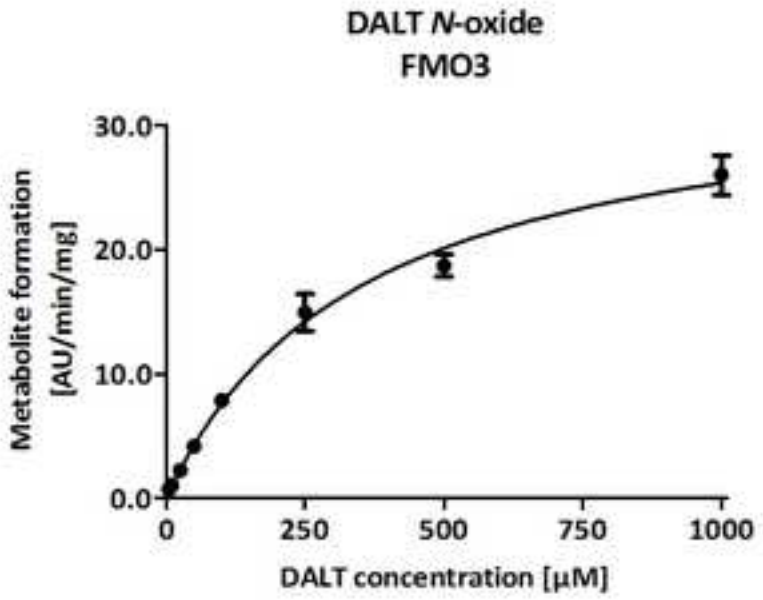

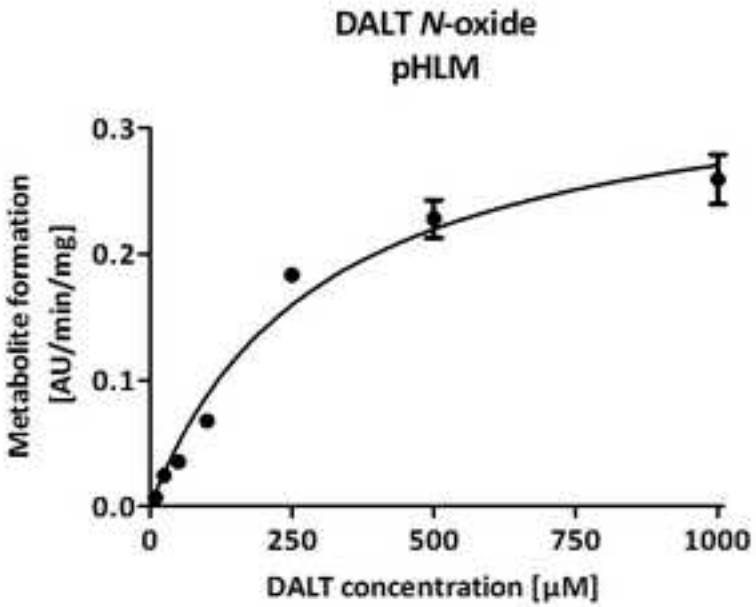

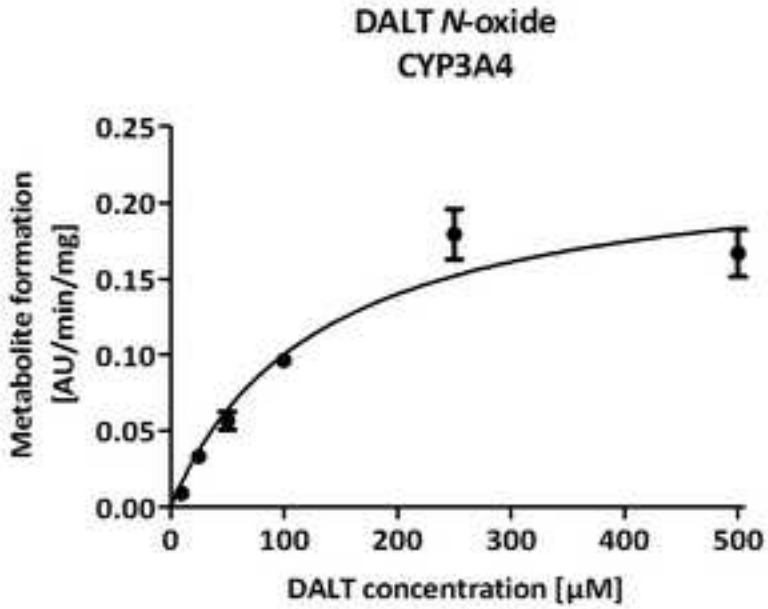

Figure 4

Click here to download high resolution image

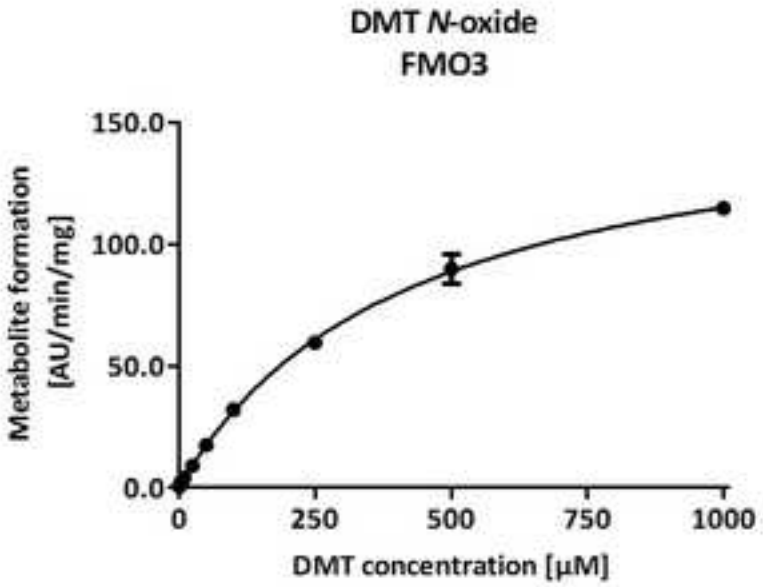

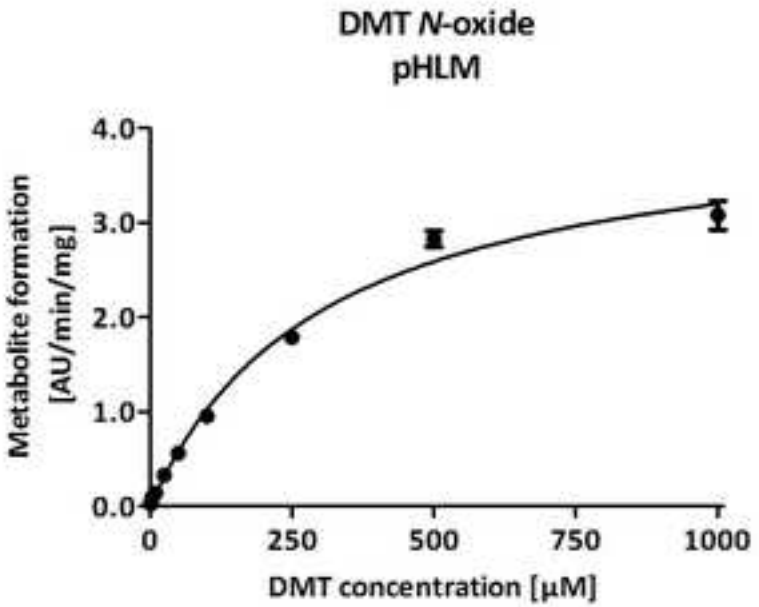

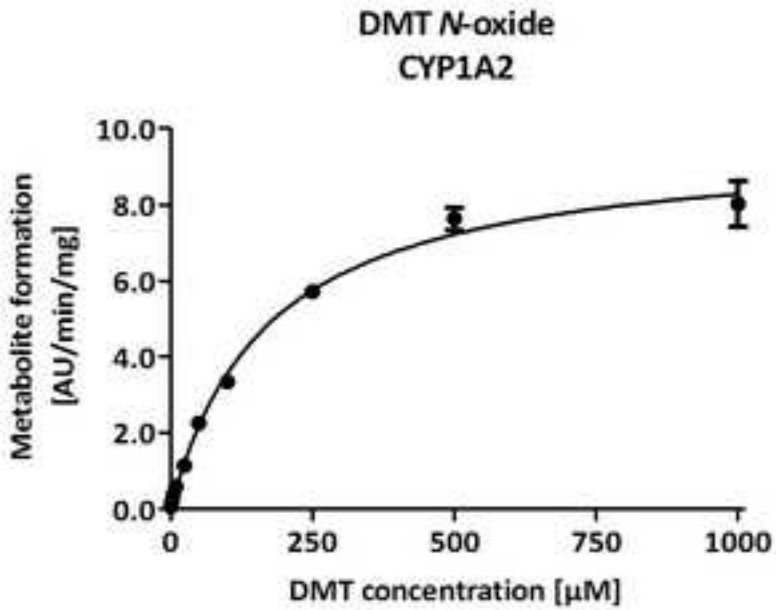

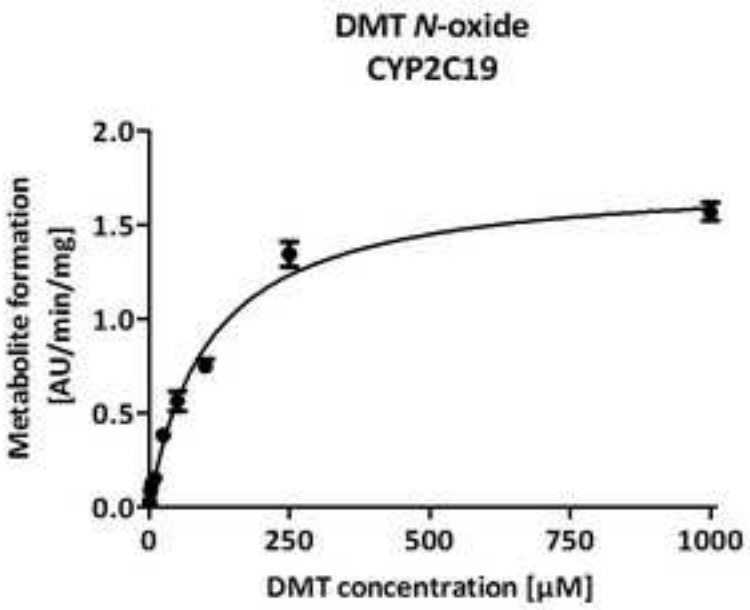

Figure 4

Click here to download high resolution image

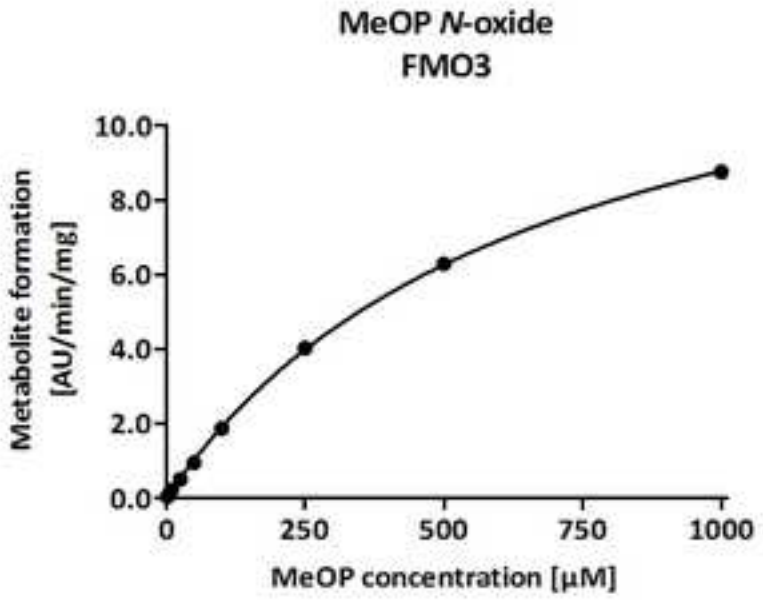

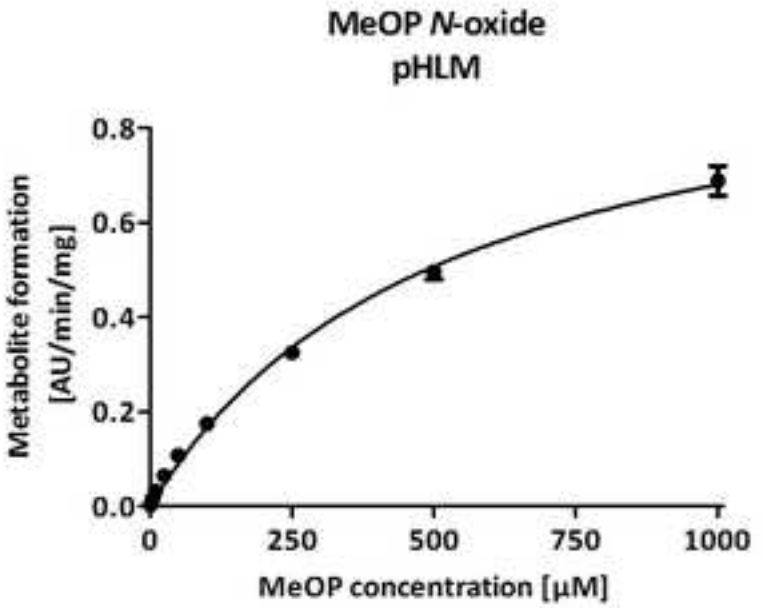

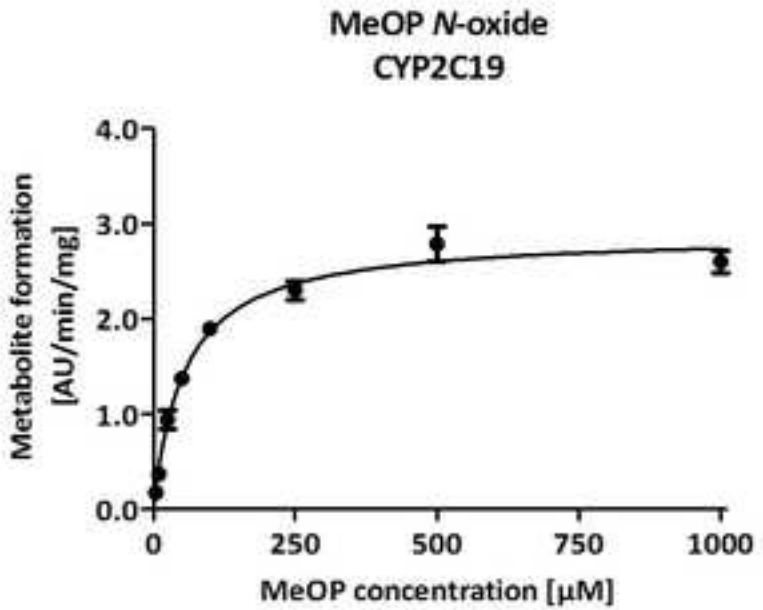

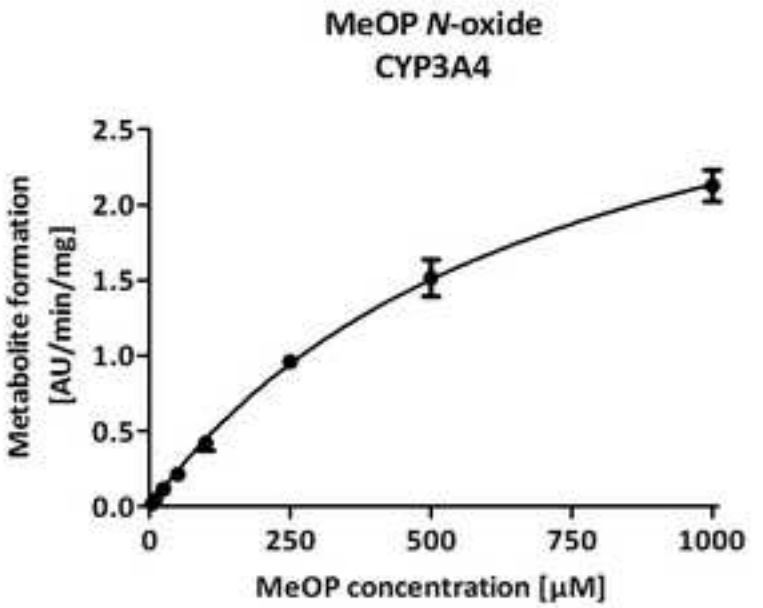

Figure 4
Click here to download high resolution image

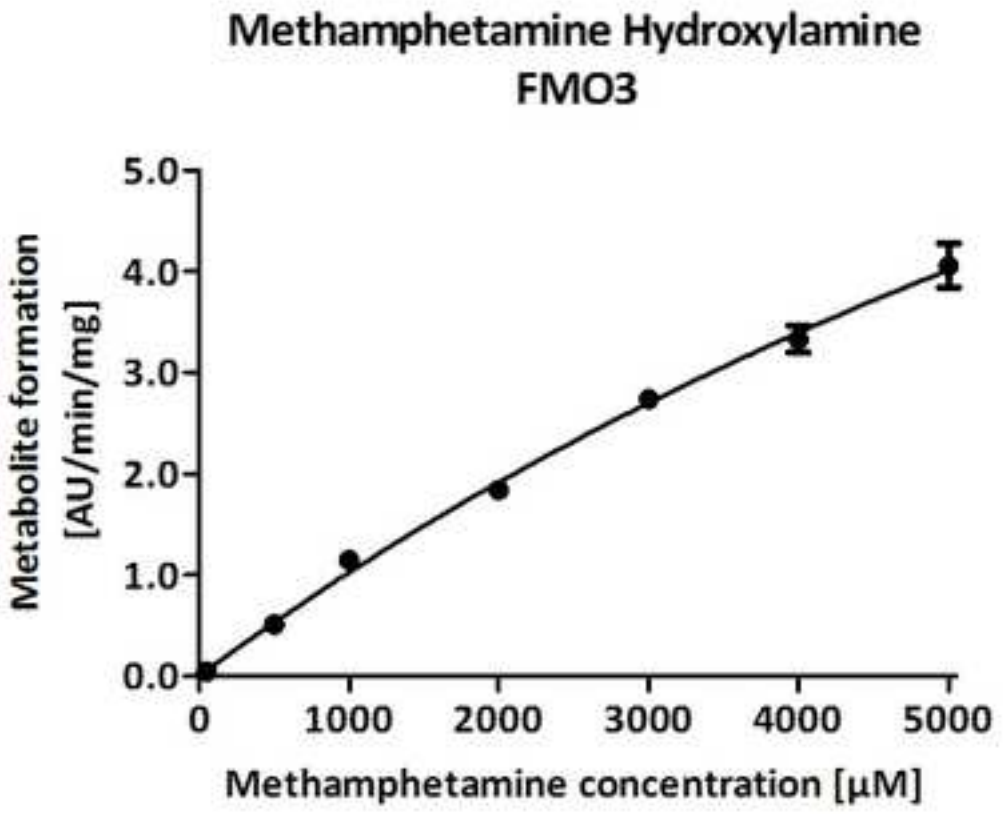

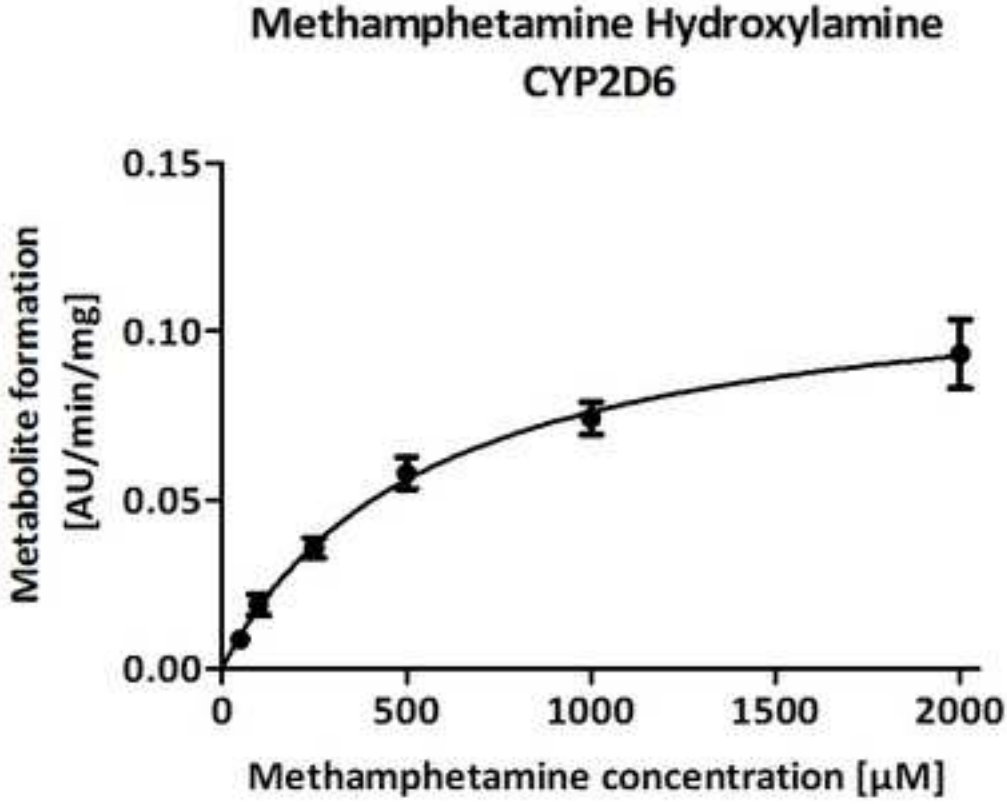

Figure 5

Click here to download high resolution image

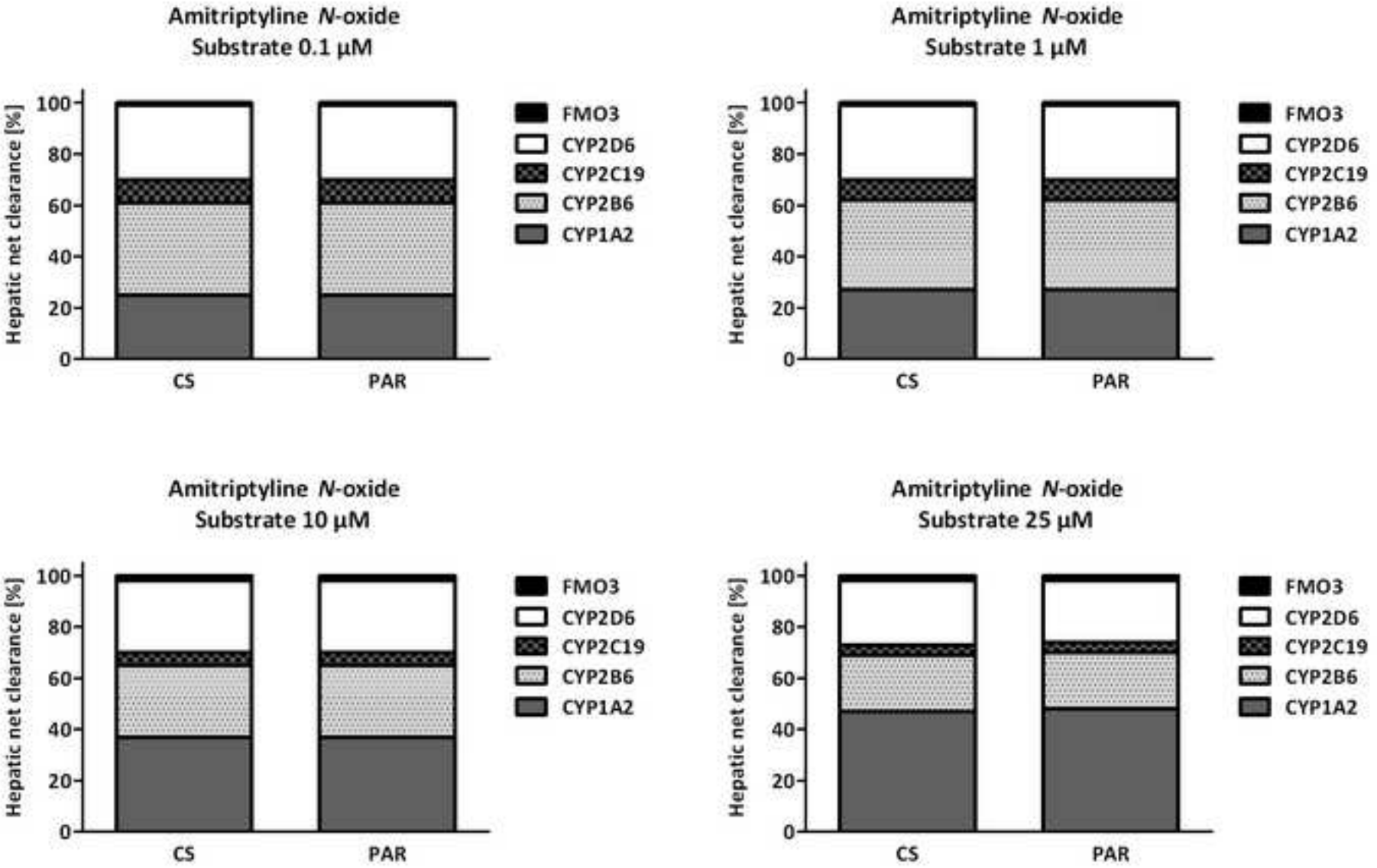

Figure 6

Click here to download high resolution image

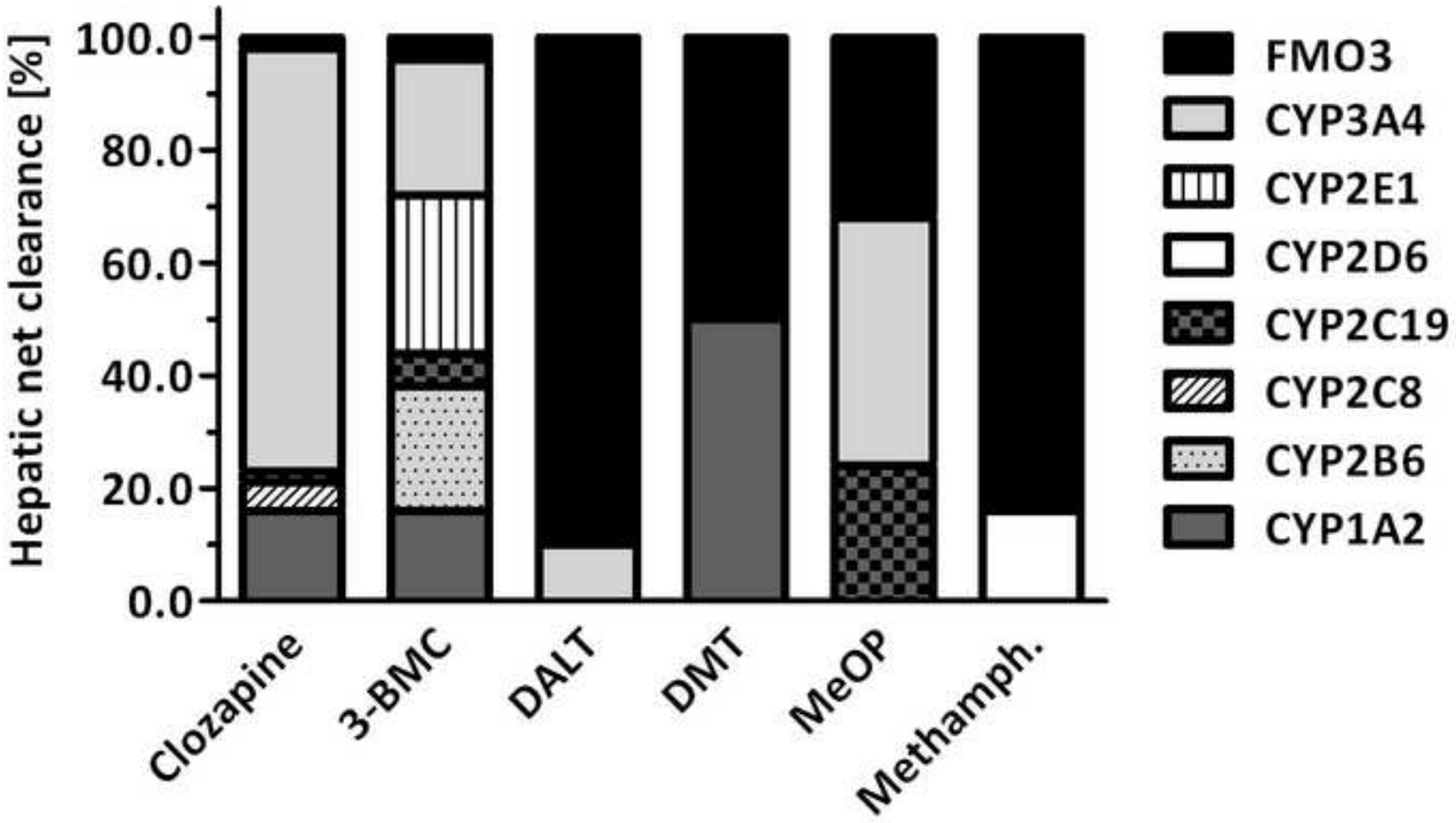

Figure 7

Click here to download high resolution image